CHAPTER FIVE

Nonideal Behavior of Components

In this chapter we will discuss the typical circuit components used in the design of electronic systems and particularly in digital electronics. Our concentration will be on their role in suppression of radiated and conducted emissions and on their *nonideal* behavior. The latter is critical to their ability to provide adequate suppression. The reader must begin to think in terms not only of the component's *ideal* behavior but also of its *nonideal* behavior. An example is the frequency response of a capacitor's impedance. These components are often used to bypass or divert a high-frequency signal from, for example, a cable where the signal may radiate very efficiently. If the desired frequency of the emission is above the *self-resonant frequency* of the capacitor, the behavior of the capacitor will resemble that of an inductor, and the low impedance desired will not be realized.

Throughout this and later chapters it is critical for the reader to remember: *the primary frequencies of interest are those of the applicable governmental regulations.* For example, if the product is intended to be marketed in the United States, the emissions in the frequency range of the FCC limits (150 kHz–30 MHz for conducted emissions and 30 MHz–40 GHz for radiated emissions) are the *primary* frequencies of interest. A radiated emission occurring at 29 MHz is of no consequence in meeting the FCC regulatory limits! However, we cannot be totally unconcerned about the levels of emissions that are outside the frequency ranges of the regulatory limits, since these emissions may cause interference with other products, which will result in field problems and customer complaints. *Merely satisfying the applicable regulatory requirements does not represent a complete system design from the standpoint of EMC.*

In this chapter we will develop *mathematical models* that yield considerable insight into the *nonideal behavior* of components. Certain approximations will need to be made in developing a relatively simple model. Throughout this text we

Introduction to Electromagnetic Compatibility, *Second Edition*, by Clayton R. Paul

will frequently show experimentally measured data that serve to illustrate the prediction accuracy of the models that are developed. It is important to keep in mind that *if a postulated model fails to predict experimentally observed phenomena, it is useless*!

Our interest in a component's behavior will focus on the high frequencies of the regulations where it is to be used to reduce conducted and/or radiated emissions. The ultimate test of whether a component will provide the anticipated performance at the desired frequency is to *experimentally measure the desired behavior* (*e.g., impedance*) *of the component at the desired frequency*! There exist a large number of commercially available test instruments that measure the high-frequency behavior of components. Most of these devices are computer-controllable and quite simple to use. One can therefore quickly and accurately determine whether a component will provide the desired EMI suppression through measurement.

5.1 WIRES

The conductors of a system (wires and printed circuit board, PCB, lands) are frequently overlooked as being important *components* of the system. If a pair of conductors is electrically long ($\mathscr{L} > \lambda/10$) at the frequency of interest, then the line behaves as a transmission line (see Chapter 4) and cannot be modeled as a lumped circuit with any degree of success. If, on the other hand, the line is electrically short at the frequency of interest, then a lumped-circuit model of it will provide adequate prediction. Their behavior at the regulatory frequencies will be our primary concern here. In the radiated emission range (30 MHz–40 GHz) and to a lesser degree in the conducted emission range (150 kHz–30 MHz), the behavior of these elements is far from the ideal. Perhaps the most important effect, at least in digital circuits, is the conductor *inductance.* The resistance of the conductors is generally more important in the functional design as in determining the required land size and/or wire gauge to ensure minimum voltage drop along them in a power distribution circuit. However, *at the frequencies of the regulatory limits and particularly in the radiated emission range the inductance of the conductors is considerably more important than the resistance.* We examine these topics in this section.

The term *wire* will be used in this text to refer to conductors that consist of one or more *solid, circular, cylindrical conductors.* A single conductor is referred to as a *solid wire.* The wire has radius r_w and conductivity σ. The vast majority of conductor materials are copper (Cu), which has a conductivity $\sigma_{\text{Cu}} = 5.8 \times 10^7\ \text{S/m}$. Normally the conductor is not ferromagnetic, and as such its permeability μ is that of free space: $\mu = \mu_0 = 4\pi \times 10^{-7}\ \text{H/m}$. Also, the permittivity of virtually all conductors is that of free space: $\epsilon = \epsilon_0 \cong (1/36\pi) \times 10^{-9}\ \text{F/m}$. Table 5.1 gives the relative conductivities (relative to Cu) σ_r and relative permeabilities (relative to free space) μ_r for various conducting materials.

Stranded wires are composed of several strands of solid wires of radii r_{ws} that are placed parallel to each other to give flexibility. *As a reasonable approximation, the resistance and internal inductance of a stranded wire consisting of S strands can be computed by dividing the resistance or internal inductance of a single strand of radius r_{ws} by the number of strands S.* Thus we are essentially treating the stranded

TABLE 5.1 Conductivities (Relative to Copper) and Permeabilities (Relative to Free Space) of Conductors

Conductor	σ_r	μ_r
Silver	1.05	1
Copper—annealed	1.00	1
Gold	0.70	1
Aluminum	0.61	1
Brass	0.26	1
Nickel	0.20	600
Bronze	0.18	1
Tin	0.15	1
Steel (SAE 1045)	0.10	1000
Lead	0.08	1
Monel	0.04	1
Stainless steel (430)	0.02	500
Zinc	0.32	1
Iron	0.17	1000
Beryllium	0.10	1
Mu-metal (at 1 kHz)	0.03	30,000
Permalloy (at 1 kHz)	0.03	80,000

wire as being S identical wires that are connected, electrically, in *parallel. The external parameters of inductance and capacitance can be approximately computed by replacing the stranded wire with a solid wire of equivalent radius.* Consequently, we can obtain the parameters we will need by considering only solid wires.

Numerous handbooks from wire manufacturers list not only the radius and number of strands of stranded wires but also list an equivalent *gauge* that roughly represents the overall radius of the bundle of strands. Wires are referred to by *gauge*, which represents a solid wire of certain radius. Although there are several gauge definitions, the most common is the *American Wire Gauge* (AWG). Manufacturer handbooks also list the wire radius corresponding to the various wire gauges. Wire radii are typically given in the English unit system in terms of *mils*, where 1 mil $= \frac{1}{1000}$ in. $= 0.001$ in. Table 5.2 gives the wire *diameters* for typical wire gauges.

Stranded wires are specified in terms of a diameter equivalent to a corresponding solid wire. Stranded wires are also specified in terms of the number and gauge of the solid wires that make up the stranded wire as (number $\times$ gauge). It is a simple matter to convert wire radii in mils to wire radii in meters. For example, the radius of a 20 AWG solid wire is $r_w = 16$ mils. To convert this to meters, we multiply by unit ratios as described in Chapter 1:

$$\begin{aligned} r_w &= 16 \text{ mils} \times \frac{1 \text{ inch}}{1000 \text{ mils}} \times \frac{2.54 \text{ cm}}{1 \text{ inch}} \times \frac{1 \text{ m}}{100 \text{ cm}} \\ &= 16 \text{ mils} \times (2.54 \times 10^{-5} \text{ m/mil}) \\ &= 0.4064 \text{ mm} \end{aligned}$$

Therefore, *to convert wire radii from mils to meters, multiply by* 2.54×10^{-5}.

TABLE 5.2 Wire Gauges (AWG) and Wire Diameters

	Wire Diameter (mils)	
Wire Gauge	Solid	Stranded
4/0	460.1	522.0 (427 × 23)
		522.0 (259 × 21)
3/0	409.6	464.0 (427 × 24)
		464.0 (259 × 23)
2/0	364.8	414.0 (259 × 23)
		414.0 (133 × 20)
1/0	324.9	368.0 (259 × 24)
		368.0 (133 × 21)
1	289.3	328.0 (2109 × 34)
		328.0 (817 × 30)
2	257.6	292.0 (2646 × 36)
		292.0 (665 × 30)
4	204.3	232.0 (1666 × 36)
6	162.0	184.0 (1050 × 36)
		184.0 (259 × 30)
8	128.5	147.0 (655 × 36)
10	101.9	116.0 (105 × 30)
		115.0 (37 × 26)
12	80.0	95.0 (165 × 34)
		96.0 (7 × 20)
14	64.1	73.0 (105 × 30)
		73.0 (41 × 30)
		73.0 (7 × 22)
16	50.8	59.0 (105 × 36)
		59.0 (26 × 30)
		60.0 (7 × 24)
18	40.3	47.0 (65 × 36)
		49.0 (19 × 30)
		47.0 (16 × 30)
		48.0 (7 × 26)
20	32.0	36.0 (41 × 36)
		36.0 (26 × 34)
		37.0 (19 × 32)
		35.0 (10 × 30)
22	25.3	30.0 (26 × 36)
		31.0 (19 × 34)
		30.0 (7 × 30)
24	20.1	23.0 (41 × 40)
		24.0 (19 × 36)
		23.0 (10 × 34)
		24.0 (7 × 32)
26	15.9	19.0 (7 × 34)

(*continued*)

TABLE 5.2 *Continued*

	Wire Diameter (mils)	
Wire Gauge	Solid	Stranded
		20.0 (19 × 38)
		21.0 (10 × 36)
28	12.6	16.0 (19 × 40)
		15.0 (7 × 36)
30	10.0	12.0 (7 × 38)
32	8.0	8.0 (7 × 40)
34	6.3	7.5 (7 × 42)
36	5.0	6.0 (7 × 44)
38	4.0	

Wires are normally covered with a cylindrical dielectric insulation for obvious reasons. The thickness of the dielectric insulation is typically of the order of the wire radius. There are various types of dielectric insulations used by wire manufacturers. Their handbooks list the dc (or low-frequency) values of relative permittivity ϵ_r for the various insulation materials. Table 5.3 lists ϵ_r for various insulation materials.

TABLE 5.3 Relative Permittivities of Insulation Dielectrics

Material	ϵ_r
Air	1.0005
Styrofoam	1.03
Polyethylene foam	1.6
Cellular Polyethylene	1.8
Teflon	2.1
Polyethylene	2.3
Polystyrene	2.5
Silicone rubber	3.1
Nylon	3.5
Polyvinyl chloride (PVC)	3.5
Epoxy resin	3.6
Quartz (fused)	3.8
Glass (pyrex)	4.0
Epoxy glass (PCB substrate)	4.7
Bakelite	4.9
Mylar	5.0
Porcelain	6.0
Neoprene	6.7
Polyurethane	7.0
Silicon	12.0

It is important to remember that *dielectric materials are not ferromagnetic and thus have relative permeabilities of free space*, $\mu_r = 1$. Therefore *wire insulations do not affect magnetic field properties caused by currents of the wires.*

5.1.1 Resistance and Internal Inductance of Wires

The dc resistance of a round wire of radius r_w, conductivity σ, and total length $\mathscr{L}$ is given by

$$R = \frac{\mathscr{L}}{\sigma \pi r_w^2} \quad \Omega \tag{5.1}$$

As the frequency is increased, the current over the wire cross section tends to crowd closer to the outer periphery because of a phenomenon known as *skin effect.* Essentially, the current can be assumed to be concentrated in an annulus at the wire surface of thickness equal to the skin depth [1]

$$\begin{aligned} \delta &= \frac{1}{\sqrt{\pi f \mu_0 \sigma}} \\ &= \frac{6.6 \times 10^{-2}}{\sqrt{f}} \quad \text{m} \\ &= \frac{2.6 \times 10^{3}}{\sqrt{f}} \quad \text{mils} \end{aligned} \tag{5.2}$$

when the skin depth is less than the wire radius. Table 5.4 gives the skin depth of copper ($\sigma = 5.8 \times 10^7$ S/m, $\epsilon_r = 1$, $\mu_r = 1$) at various frequencies.

Note that the skin depth becomes extremely small at frequencies in the range of the radiated emission regulatory limits. At roughly the middle of this band, 100 MHz, the skin depth is 0.26 mils. Current tends to be predominantly concentrated in a strip near the surface of a conductor of depth δ. Therefore a conductor carrying a high-frequency current utilizes only a very small fraction of the metal of that conductor.

TABLE 5.4 Skin Depth of Copper

f	δ
60 Hz	8.5 mm
1 kHz	2.09 mm
10 KHz	0.66 mm
100 kHz	0.21 mm
1 MHz	2.6 mils
10 MHz	0.82 mils
100 MHz	0.26 mils
1 GHz	0.0823 mils

Figure 5.1 illustrates the fact that the current in a round wire is uniformly distributed over the cross section at dc, but is increasingly concentrated in a narrow thickness of approximately one skin depth near the outer surface for higher frequencies. Since the resistance is proportional to cross-sectional area occupied by the current, the *per-unit-length* resistance becomes

$$\begin{aligned} r_{\text{lf}} &= r_{\text{dc}} \quad \text{for } r_w \ll \delta \\ &= \frac{1}{\sigma \pi r_w^2} \quad (\text{in } \Omega/\text{m}) \\ r_{\text{hf}} &= \frac{1}{\sigma[\pi r_w^2 - \pi(r_w - \delta)^2]} \quad \text{for } r_w \gg \delta \qquad (5.3a) \\ &\cong \frac{1}{\sigma 2\pi r_w \delta} \\ &= \frac{r_w}{2\delta} r_{\text{dc}} \\ &= \frac{1}{2r_w}\sqrt{\frac{\mu_0}{\pi\sigma}}\sqrt{f} \quad (\text{in } \Omega/\text{m}) \qquad (5.3b) \end{aligned}$$

This is plotted in Fig. 5.1. Observe from (5.2) that the skin depth decreases with increasing frequency as the inverse square root of the frequency, $\sqrt{f}$. Thus the

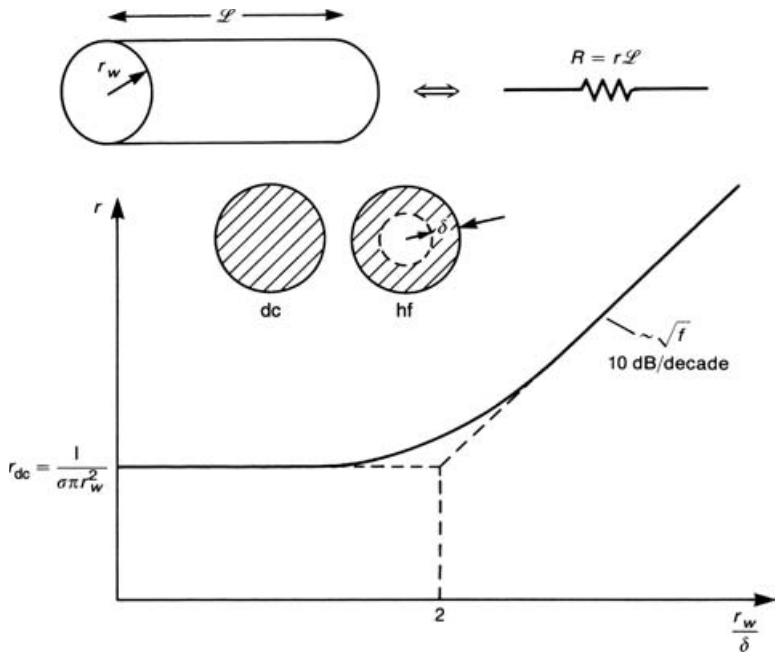

FIGURE 5.1 Illustration of the dependence of the per-unit-length resistance of a wire on frequency (skin effect).

high-frequency resistance r_{hf} increases at a rate of 10 dB/decade. The resistance remains at the dc value up to the frequency where these two asymptotes meet, or $r_w = 2\delta$. The resistance in (5.3) is a *per-unit-length* resistance, with units of Ω/m. A length $\mathscr{L}$ of wire would have a total resistance $R = r\mathscr{L}$.

The isolated wire also has an inductance that is frequency-dependent. This is referred to as the *internal inductance*, since it is due to magnetic flux internal to the wire. The *dc internal inductance* is derived in [1] as

$$\begin{aligned} l_{i,\,\text{dc}} &= \frac{\mu_0}{8\pi} \quad \text{for } r_w \ll \delta \\ &= 0.5 \times 10^{-7} \text{ H/m} \\ &= 50 \text{ nH/m} \\ &= 1.27 \text{ nH/in.} \end{aligned} \tag{5.4a}$$

This is also a *per-unit-length* parameter. A length $\mathscr{L}$ of conductor would have a total internal inductance $L_i = l_i\mathscr{L}$. For high-frequency excitation the current again tends to crowd toward the wire surface, and tends to be concentrated in a thickness δ. The per-unit-length internal inductance for these higher frequencies is also derived in [1], and becomes

$$\begin{aligned} l_{i,\,\text{hf}} &= \frac{2\delta}{r_w} l_{i,\,\text{dc}} \quad \text{for } r_w \gg \delta \\ &= \frac{1}{4\pi r_w}\sqrt{\frac{\mu_0}{\pi\sigma}}\frac{1}{\sqrt{f}} \end{aligned} \tag{5.4b}$$

Since the skin depth δ decreases with increasing frequency as the inverse square root of the frequency, (5.4b) shows that the high-frequency, per-unit-length internal inductance *decreases* at the rate of -10 dB/decade for $r_w \gg \delta$. This frequency behavior is plotted in Fig. 5.2.

Example 5.1 Determine the resistance and internal inductance of a 2 in. length of 20-gauge solid copper wire at 200 MHz.

***Solution*:** First we determine whether the wire radius is in the dc region on the skin effect region of Fig. 5.1. The skin depth at 200 MHz is

$$\begin{aligned} \delta &= \frac{1}{\sqrt{\pi f \mu_0 \sigma}} \\ &= \frac{1}{\sqrt{\pi \times 2 \times 10^8 \times 4\pi \times 10^{-7} \times 5.8 \times 10^7}} \\ &= 4.67 \times 10^{-6} \text{ m} \\ &= 0.184 \text{ mils} \end{aligned}$$

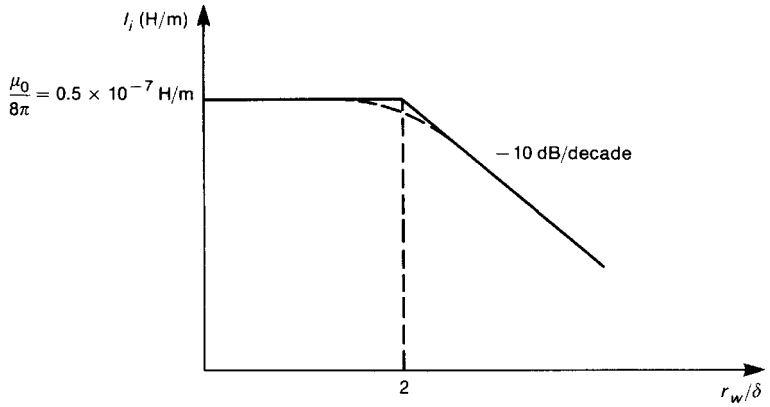

FIGURE 5.2 Illustration of the dependence of the per-unit-length internal inductance of wires on frequency (skin effect).

The radius of a 20-gauge solid wire is, from Table 5.2, 16 mils. Hence we are in the skin effect region since $r_w \gg \delta$. Thus we compute the per-unit-length resistance from (5.3b) as

$$\begin{aligned} r_{\text{hf}} &= \frac{1}{2r_w}\sqrt{\frac{\mu_0}{\pi\sigma}}\sqrt{f} \\ &= \frac{1}{2 \times 16 \times 2.54 \times 10^{-5}}\sqrt{\frac{4\pi \times 10^{-7}}{\pi \times 5.8 \times 10^{7}}}\sqrt{2 \times 10^{8}} \\ &= 1.44\ \Omega/\text{m} \\ &= 36.7\ \text{m}\Omega/\text{in.} \end{aligned}$$

Hence the total resistance is

$$\begin{aligned} R &= r_{\text{hf}} \times \mathscr{L} \\ &= 73.4\ \text{m}\Omega \end{aligned}$$

The internal inductance is computed from (5.4b) as

$$\begin{aligned} l_{i,\,\text{hf}} &= \frac{1}{4\pi r_w}\sqrt{\frac{\mu_0}{\pi\sigma}}\frac{1}{\sqrt{f}} \\ &= \frac{r_{\text{hf}}}{2\pi f}\frac{1}{} \\ &= 1.15\ \text{nH/m} \\ &= 29.2\ \text{pH/in.} \end{aligned}$$

The total internal inductance is

$$\begin{aligned} L_{i,\,\mathrm{hf}} &= l_{i,\,\mathrm{hf}} \times \mathscr{L} \\ &= 58.4 \text{ pH} \end{aligned}$$

5.1.2 External Inductance and Capacitance of Parallel Wires

The resistance and internal inductance derived previously are uniquely attributable to or associated with a wire. Currents require a return path. The most common configuration is a pair of parallel wires of equal radii r_w, length $\mathscr{L}$, and separation s, as shown in Fig. 5.3. The magnetic flux external to each wire contributes to the total flux penetrating the area between the two wires. The per-unit-length *external inductance* l_e of a pair of wires is the ratio of the magnetic flux between the two wires ψ_m, per unit of line length to the current producing that flux. This was derived in Chapter 4, and, assuming that the wires are separated sufficiently ($s/r_w > 5$) such that the current is uniformly distributed around the wire peripheries so that *proximity effect* is not a factor, is given as

$$\begin{aligned} l_e &= \frac{\psi_m/\mathscr{L}}{I} \\ &= \frac{\mu_0}{\pi} \ln\left(\frac{s}{r_w}\right) \text{ (in H/m)} \\ &= 0.4 \ln\left(\frac{s}{r_w}\right) \text{ (in } \mu\text{H/m)} \\ &= 10.16 \ln\left(\frac{s}{r_w}\right) \text{ (in nH/in.)} \end{aligned} \tag{5.5}$$

The total *loop inductance* is the sum of the product of the line length and the internal inductances of the two wires and the product of the per-unit-length external inductance and the line length, i.e., $L_{\text{loop}} = 2l_i\mathscr{L} + l_e\mathscr{L}$. Note that $l_e\mathscr{L}$ is the inductance of the loop bounded by the two wires. Observe that the external inductance is a loop inductance and may be assigned to either wire in the loop.

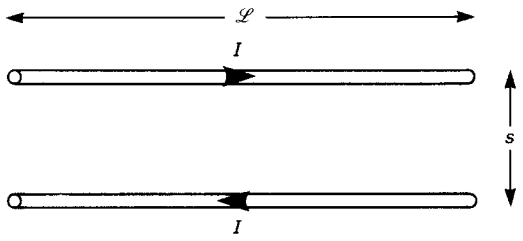

FIGURE 5.3 A pair of parallel wires to be modeled with an equivalent circuit.

Charge on the wires contributes to a *per-unit-length capacitance* c between the two wires that depends on the wire separation and radii, as did the external inductance. This *per-unit-length capacitance* was derived in Chapter 4, and is the ratio of the per-unit-length charge on the wires, $Q/\mathscr{L}$, to the voltage between them:

$$\begin{aligned} c &= \frac{Q/\mathscr{L}}{V} \\ &= \frac{\pi\epsilon_0}{\ln(s/r_w)} \quad \text{(in F/m)} \\ &= \frac{27.78}{\ln(s/r_w)} \quad \text{(in pF/m)} \\ &= \frac{0.706}{\ln(s/r_w)} \quad \text{(in pF/in.)} \end{aligned} \tag{5.6}$$

This result assumes that the wires are separated sufficiently ($s/r_w > 5$) such that the charge is uniformly distributed around the wire peripheries and *proximity effect* is not a factor. The total capacitance between a pair of parallel wires of total length $\mathscr{L}$ is the product of the per-unit-length capacitance and the line length: $C = c\mathscr{L}$.

Review Exercise 5.1 Determine the per-unit-length inductance and capacitance of two 20-gauge, solid parallel wires separated by $\frac{1}{4}$ in.

***Answers*:** 27.9 nH/in. and 0.257 pF/in.

5.1.3 Lumped Equivalent Circuits of Parallel Wires

Each of these per-unit-length parameters when multiplied by the length gives the total parameter for that length of line. If the total line length $\mathscr{L}$ is *electrically short*, i.e., $\mathscr{L} \ll \lambda$, at the frequency of excitation, we may lump these distributed parameters and obtain *lumped equivalent circuits* of the pair of wires. On the other hand, if the line is electrically long ($\mathscr{L} > \lambda$), then we have no recourse but to model the line as a transmission line (Chapter 4). Combining these elements gives several possible lumped-circuit models of the pair of parallel wires shown in Fig. 5.4. The *lumped-backward gamma* model of Fig. 5.4a is so named because of its resemblance to the Greek letter Γ. The remaining lumped-circuit models, *lumped-Pi*, *lumped-T*, and *lumped-*Γ *models* in the remaining parts of the figure are similarly named. Either of these models would constitute acceptable approximations of the line so long as the line is electrically short. However, depending on the impedance level of the load attached to the endpoint of the wires, one model will extend the prediction accuracy of the model further in frequency than another model. This is discussed and investigated in [2]. For example, if the load

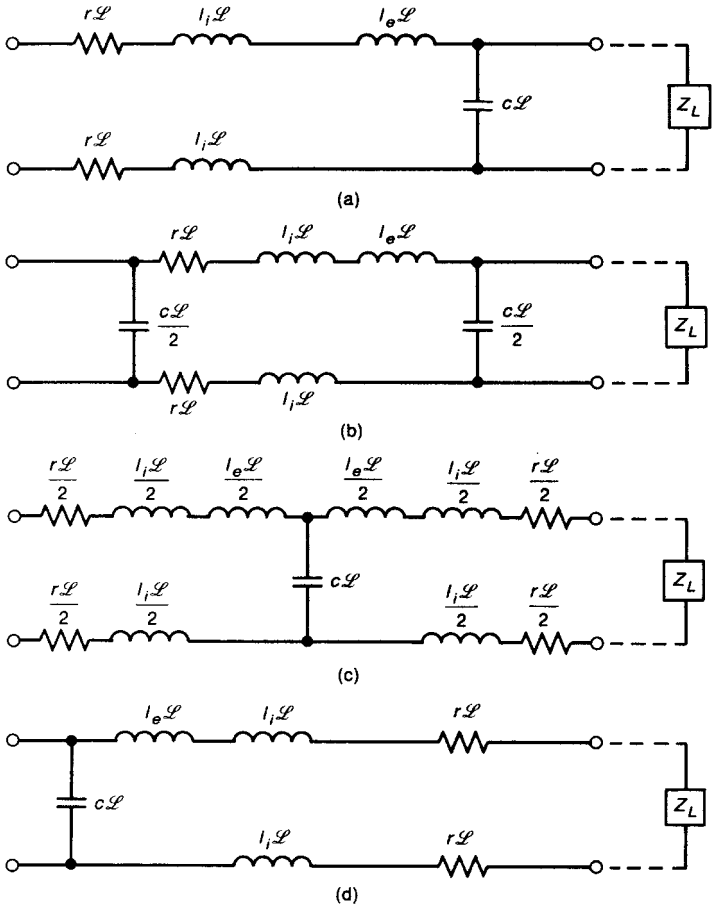

FIGURE 5.4 Lumped equivalent circuits for a pair of parallel wires: (a) lumped-backward Γ; (b) lumped Pi; (c) lumped T; (d) lumped Γ.

impendence Z_L is a "low impedance," i.e., much less than the *characteristic impedance* of the line

$$Z_C = \sqrt{\frac{l_e}{c}}$$
$$= 120 \ln\left(\frac{s}{r_w}\right) \quad \Omega \tag{5.7}$$

the lumped-Γ model of Fig. 5.4(d) and the lumped-T model of Fig. 5.4(c) would extend the frequency range of adequate prediction slightly higher than the lumped-backward gamma and lumped-Pi models of Fig. 5.4a, b. This is intuitively

reasonable because a low impedance load would be in parallel with the rightmost parallel capacitance element of the lumped-backward gamma and lumped-Pi models. Thus these elements will be rendered ineffective by the low impedance load. The converse applies to high-impedance loads; the rightmost resistance and inductance elements of the lumped-Γ and lumped-T models are in series with this high-impedance load, and are therefore rendered ineffectual.

Once the per-unit-length parameters of the wires are determined and these lumped circuits are constructed, any lumped-circuit analysis program such as SPICE can be used to analyze the resulting circuit with the loads (gates, etc.) attached. Important time-domain parameters such as risetime, waveshape, and time delay can be easily determined from that simulation.

An important point concerning these models that is frequently misunderstood needs to be discussed. Note that in either of the lumped circuits in Fig. 5.4 the external inductance l_e is in series with the internal inductance l_i. The impedance of the external inductance is $\omega L_e = 2\pi f l_e \mathscr{L}$, and therefore increases directly with frequency. (The external inductance is approximately frequency-independent.) The impedance of the internal inductance is $\omega L_i = 2\pi f l_i \mathscr{L}$ and also appears to increase directly with frequency. However, on closer examination, we recall that the per-unit-length internal inductance decreases with increasing frequency as the inverse square root of the frequency. Thus *the impedance of the internal inductance increases only as the square root of the frequency.* Therefore the impedance of the external inductance increases with frequency at a rate faster than that of the impedance of the internal inductance! Also, the external inductance for typical wire sizes and separations is usually much larger than the internal inductance. For example, consider a pair of 20-gauge solid copper wires that are separated by a distance of 50 mils (typical separation between adjacent conductors in a ribbon cable). The per-unit-length internal inductance is $l_{i,\mathrm{dc}} = 0.05\,\mu\mathrm{H/m} = 1.27\,\mathrm{nH/in.}$, whereas the per-unit-length external inductance is $l_e = 0.456\,\mu\mathrm{H/m} = 11.58\,\mathrm{nH/in.}$, which is larger than the internal inductance by a factor of 10! Consider higher frequencies where $r_w > 2\delta$. The per-unit-length external inductance is larger than the per-unit-length internal inductance by a factor of 10, and above this frequency the difference increases since the external inductance remains constant with increasing frequency but the internal inductance decreases as $1/\sqrt{f}$. Consequently, *the impedance of the internal inductance is usually much smaller than the impedance of the external inductance, and we may therefore neglect the internal inductance in the model.* It is important to make these types of observations where possible based on typical dimensions in order to obtain the simplest model so that qualitative behavior can be more easily extracted from the model.

Several final points need to be discussed. In the above derivations of the per-unit-length external parameters l_e and c we assumed that the medium surrounding the wires was *homogeneous* and was that of free space with permittivity ϵ_0 and permeability μ_0. Thus we assumed *bare wires in free space.* Wires often have circular dielectric insulation surrounding them to prevent contact with other wires. This type

of medium is said to be *inhomogeneous*, since the electric and magnetic fields exist partly in the dielectric insulations (ϵ_r) and partly in air. Dielectrics are not ferromagnetic, and thus have $\mu = \mu_0$. Thus *the presence of inhomogeneous dielectric media does not affect the external inductance parameter.* However, since the surrounding medium is inhomogeneous in permittivity ϵ, Eq. (5.6) for the per-unit-length capacitance of the line *does not apply.* We cannot simply replace ϵ_0 in that equation with the permittivity of the dielectric insulation, since the electric fields are not confined to the dielectric. Derivation of the per-unit-length capacitance for an inhomogeneous medium is a difficult problem, and closed-form expressions do not exist for this case—contrary to what some handbooks imply. Numerical methods must be applied in this case [3]. In spite of these technicalities, *we can obtain reasonable approximations for the inhomogeneous medium case ignoring the dielectric insulations* and using the preceding expressions for l_e, (5.5), c, (5.6), for typical wire sizes, dielectric insulation thicknesses, and wire separations.

Review Exercise 5.2 Compute the total internal and external inductances, resistance, and capacitance for a pair of 28-gauge, solid wires that are 5 in. in length and separated by 50 mils at a frequency of 10 MHz.

***Answers*:** 0.209 Ω, 3.32 nH, 105 nH, 1.7 pF.

5.2 PRINTED CIRCUIT BOARD (PCB) LANDS

Wires are generally found in cables that interconnect subsystems and PCBs within systems. The conductors on PCBs have rectangular cross sections, as opposed to wires, whose cross sections are circular. PCBs are composed of a dielectric substrate (typically glass epoxy with $\epsilon_r \cong 4.7$) on which rectangular cross-section conductors (*lands*) are etched. Typical board thicknesses are of order 47–62 mils. Land thicknesses are specified in terms of the thickness of the board cladding that was etched away to form the lands. Typical cladding thicknesses are 1 ounce Cu and 2 ounce Cu. This refers to the weight of that thickness of the copper material that occupies an area of one square foot. For example, the thickness of 1 ounce Cu cladding is 1.38 mils, and a 1 ft^2 area would weigh l ounce. The thickness of 2 ounce Cu is double this, or 2.76 mils. Throughout this text we will assume the most common thickness of 1 ounce Cu or 1.38 mils.

The current distribution over the land cross section behaves in a manner that is quite similar to that of wires. For dc or low-frequency excitation the current is approximately uniformly distributed over the land cross section as illustrated in Fig. 5.5. Thus the per-unit-length low-frequency resistance of the land is

$$r_{\text{lf}} = r_{\text{dc}} = \frac{1}{\sigma wt} \quad (\text{in } \Omega/\text{m}) \tag{5.8a}$$

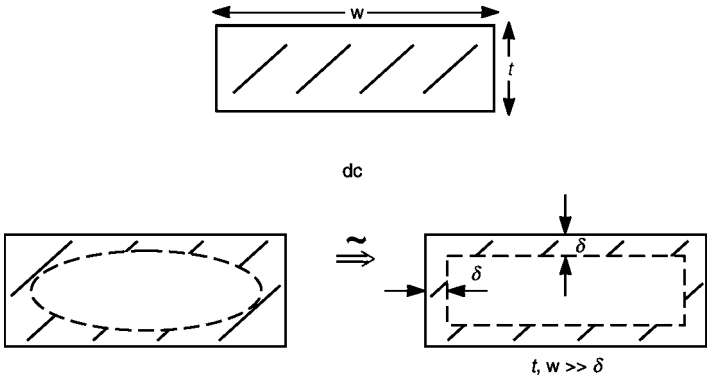

FIGURE 5.5 Illustration of skin effect for PCB lands.

where w is the land width and t is the thickness (1.38 mils). For high-frequency excitation the current tends to crowd to the outer edges of the land as illustrated in Fig. 5.5. Calculation of the high-frequency resistance is a difficult problem, but can be reasonably approximated by assuming that the current is uniformly distributed over a skin depth δ to give

$$r_{\text{hf}} = \frac{1}{\sigma(2\delta w + 2\delta t)}$$
$$= \frac{1}{2\sigma\delta(w+t)} \quad (\text{in } \Omega/\text{m}) \tag{5.8b}$$

As derived in Section 4.5.4 of Chapter 4, the dc and high-frequency resistances in (5.8a) and (5.8b) have asymptotes that join at a frequency where

$$\delta = \frac{1}{2}\frac{wt}{(w+t)}$$
$$\cong \frac{t}{2} \qquad w \gg t \tag{5.8c}$$

Hence, above this frequency we use (5.8b) to compute the resistance.

The land also possesses an internal inductance due to magnetic flux internal to the land in a fashion similar to that of a wire. However, in the case of a land, computation of this internal inductance is a difficult problem. We will ignore this internal inductance parameter on the assumption that it will be negligible in comparison with the external inductance parameter in any lumped-circuit model.

The computation of the external inductance and capacitance of a pair of parallel lands is much more difficult than for a pair of parallel wires. Generally this can be done using only numerical methods. Approximate formulas for these configurations are developed from these numerical computations and are given in Section 4.2.2 of Chapter 4. The results are given in terms of two parameters: the characteristic

impedance of the line

$$Z_C = \sqrt{\frac{l_e}{c}} \quad \Omega \tag{5.9a}$$

and effective relative permittivity or dielectric constant ϵ_r'. The effective relative permittivity accounts for the fact that the electric field lines are partly in air and partly in the PCB board (see Fig. 4.12 of Chapter 4). From this, the velocity of propagation can be computed as

$$\begin{aligned} v &= \frac{1}{\sqrt{l_e c}} \\ &= \frac{1}{\sqrt{\epsilon_r' \epsilon_0 \mu_0}} \\ &= \frac{v_0 = 3 \times 10^8}{\sqrt{\epsilon_r'}} \quad \text{m/s} \\ &= \frac{11.8}{\sqrt{\epsilon_r'}} \quad \text{in./ns} \end{aligned} \tag{5.9b}$$

Approximate formulas for typical PCB configurations such as the stripline, the microstrip, and the PCB I and PCB II configurations are given in Section 4.2.2 of Chapter 4. The per-unit-length external inductance and capacitance can be obtained from these as

$$l_e = \frac{Z_C}{v} \tag{5.10a}$$

and

$$c = \frac{1}{v Z_C} \tag{5.10b}$$

Once these parameters are obtained along with the per-unit-length resistance, the lumped equivalent circuits of Fig. 5.4 can be constructed (neglecting the internal inductance of the conductors) for any pair of rectangular cross-section conductors mounted on or in a PCB.

Review Exercise 5.3 Determine the total resistance, external inductance, and capacitance of the PCB I line of Fig. 4.12c (of Chapter 4) whose total length is 5 in. and whose dimensions are $s = 15$ mils, $w = 15$ mils, $h = 62$ mils, $t = 1.38$ mils and $\epsilon_r = 4.7$. The frequency is 100 MHz.

***Answers*:** 796 mΩ, 102 nH, 4.89 pF.

5.3 EFFECT OF COMPONENT LEADS

We now embark on an examination of the various discrete components, resistors, capacitors, inductors, etc., that are employed in electronic systems. Our emphasis will be on their *nonideal behavior* in the high-frequency range of the regulatory limits. A component must inevitably be connected to the circuit via *leads.* These connection leads usually take the form of bare wires such as the attachment leads of resistors, capacitors, etc. This is referred to as *discrete-lead attachment.* There is an increasing use of other attachment techniques that speed automated assembly of the components on the printed circuit boards (PCBs). Perhaps the most common alternative is the *surface-mount technology* (SMT) method. With this method, flat, rectangular cross-section "tabs" attached to the component package are soldered directly to the PCB. Not only does this reduce the length of the attachment leads (an important factor in achieving the desired behavior of the component), but it also speeds the automated attachment of the component to the PCB. It also allows an increased number of components to be placed on the PCB over the discrete-lead attachment method. Components are normally placed on only one side of a PCB. With the use of SMT components, many of the smaller components such as resistors and capacitors can be placed on the other side of the PCB, thereby increasing the component density. Most PCBs in today's electronic systems could not be "populated" in the allowable board space without the use of SMT components. We will concentrate on the discrete-lead components, although many of our results will also be applicable to SMT components.

One of the most important factors that affect the high-frequency behavior of components is the *length of the component attachment leads.* Unnecessarily long attachment leads cause the component behavior to deviate from the ideal at high frequencies, which often fall in the frequency range of the regulatory limits where we want the component to behave as expected. The *length and separation of the component leads* cause the component to have, in addition to the ideal behavior, an *inductive* element and a *capacitive* element. These elements in combination with the component can give an overall behavior that is far from the desired ideal behavior.

In order to model the inductance of the attachment leads, consider the discrete lead attachment shown in Fig. 5.6a. The inductance of this loop can be obtained using the previous results by multiplying the per-unit-length inductance of the pair of parallel wires given in (5.5) by the lead length. As an example, consider typical component leads that are 20-guage solid wires ($r_w = 16$ mils). Suppose that the leads are 0.5 in. long and are separated by 0.25 in. The expression in (5.5) gives 14 nH. The equivalent circuit becomes as shown in Fig. 5.6b. The inductance we have computed is the inductance of the loop, and as such we may lump it and place it in either lead.

The next effect that we will consider is the capacitance between the leads shown in Fig. 5.7. This may be computed by multiplying the per-unit-length capacitance given in (5.6) by the lead length. As an example, consider two 20-gauge leads of length 0.5 inch separated by 0.25 inch. The capacitance is 0.128 pF.

The lumped-circuit model of lead inductance is shown in Fig. 5.6b, and the model of lead capacitance is shown in Fig. 5.7b. How shall we combine these two effects

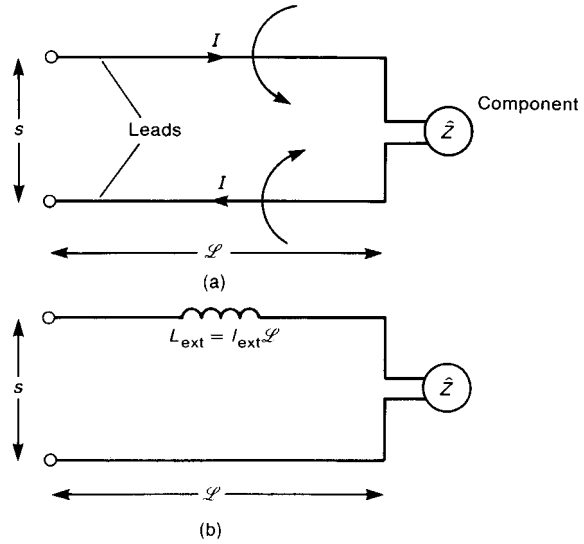

FIGURE 5.6 Modeling the effect of magnetic fields of component leads: (a) physical configuration; (b) the equivalent circuit.

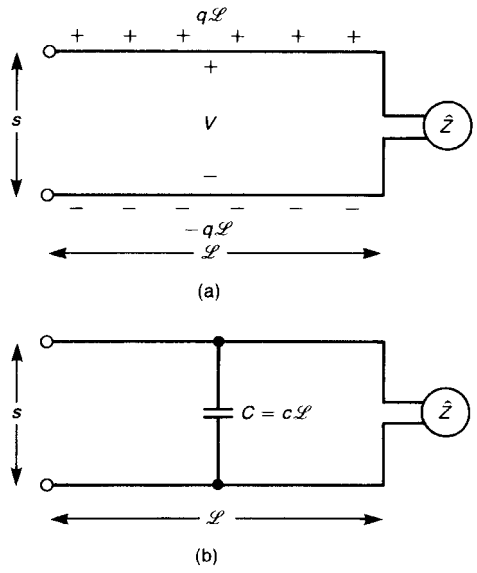

FIGURE 5.7 Modeling the effect of electric fields of component leads: (a) physical configuration; (b) the equivalent circuit.

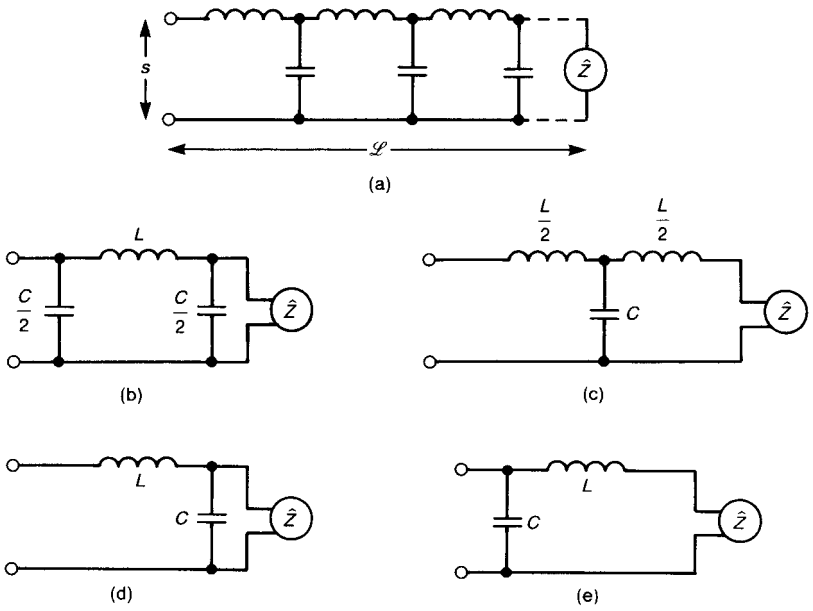

FIGURE 5.8 Equivalent circuits of component leads: (a) distributed parameter; (b) lumped Pi; (c) lumped T; (d) lumped-backward Γ; (e) lumped Γ.

into a single model? There is no unique answer to this question, since these are *distributed parameter elements.* In other words, their effects are distributed along the length of the leads, as illustrated in Fig. 5.8a.

Nevertheless, if the lead length $\mathscr{L}$ and separation s are *electrically short* at the frequencies of interest, we may lump L and C (the per-unit-length values multiplied by the lead length $\mathscr{L}$) and produce several *lumped-circuit models* that are identical in structure to those derived for the pair of parallel wires in Section 5.1.3. Figures 5.8b–e again show these four possible equivalent circuits. Again, although either circuit would be an approximate representation of this distributed-parameter phenomenon for electrically short lead lengths, one structure may be a better approximation than the other, depending on the impedance $\hat{Z}$ of the component, as was discussed in Section 5.1.3. In fact, we are interested only in estimates of the effect of the leads, and for this purpose either model would be adequate. In these models we have ignored conductor losses on the assumption that these connection leads are short, physically.

5.4 RESISTORS

Resistors are perhaps the most common component in electronic systems. These components are constructed in basically three forms: (1) carbon composition,

(2) wire wound, and (3) thin film. Carbon-composition resistors are the most common. They are constructed by forming a cylindrical block of carbon and attaching two wires to the ends. Wire-wound resistors are formed by winding a length of wire that has the desired *dc resistance* on a cylindrical form to conserve space. Wire-wound resistors have a significant amount of inductance due to the construction technique. It is usually difficult to determine whether a resistor is carbon-composition or wire-wound by simply looking at it. The desired length of the wire used to construct a wire-wound resistor can be computed from (5.1). Thin-film resistors are constructed by depositing a thin, metallic film on an insulating substrate. Leads are attached to the ends of the metallic film, and the package resembles an axial-lead resistor. Because of the construction technique, this resistor has more precise values of resistance than does the carbon-composition type but less inductance than does the wire-wound type.

The ideal frequency response of a resistor has a magnitude equal to the value of the resistor and a phase angle of 0° for all frequencies as shown in Fig. 5.9. We denote this as

$$\hat{Z} = R\underline{/0^\circ} \tag{5.11}$$

Actual resistors behave somewhat differently than this ideal at higher frequencies, with the degree to which they differ depending on the construction technique used. For example, since a wire-wound resistor is constructed of turns of wire, we would expect this resistor to have a significant inductive behavior at higher frequencies. Carbon-composition resistors would not be expected to exhibit this behavior to the same degree. Consequently, if the current passing through the resistor has a large di/dt factor, we would be well advised to use a carbon-composition resistor here instead of a wire-wound resistor. Otherwise, the wire-wound resistor would have a terminal behavior represented by $v(t) = Ri(t) + L\,di(t)/dt$. An example of where this nonideal behavior would be very undesirable would be in the use of

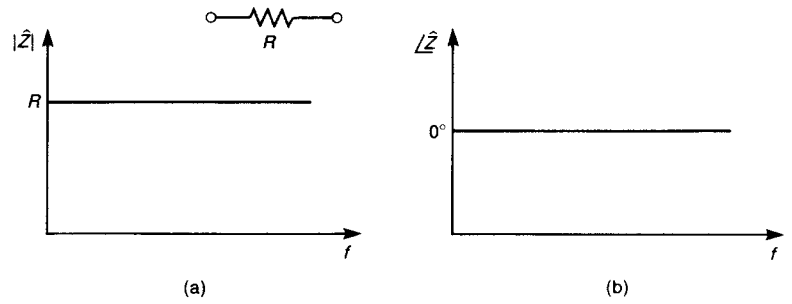

FIGURE 5.9 Frequency behavior of the impedance of an ideal resistor: (a) magnitude; (b) phase.

this resistor as a "sense resistor" in the source lead of a field-effect transistor that is used as the switch element in a switching power supply. The voltage developed across this resistor is *intended* to be a replica of the current passing out this lead of the transistor, and is used as a control to affect the duty cycle of the transistor switch. However, since the current is rapidly changing with time, the inductive nature of a wire-wound resistor may cause the voltage developed across it to resemble the derivative of this current, which would not be desirable.

The advantage of wire-wound resistors over carbon-composition ones is that much tighter tolerances on element value can be obtained. For example, carbon resistors typically have tolerances of 5–10%. This means that the manufacturer guarantees only that, for example, a 1-kΩ resistor would have a value between 1.1 kΩ and 900 Ω for a 10% tolerance. For the *sense* resistor in the abovementioned switching power supply it is important to use a small value of resistance so that the functional performance of the transistor switch will not be impaired. Typical values are of order 1 Ω. The proper operation of the switcher depends on obtaining accurate values of the sampled current, which a 10% tolerance carbon resistor may not give. Consequently a wire-wound resistor might be used in this application. From a functional standpoint, this inductive behavior of the wire-wound resistor can be tolerated. From an EMC standpoint, however, the differentiation of this switch waveform causes pulses of voltage to be developed across the resistor that have a repetition rate of the basic switch frequency *and* very fast rise/falltimes. We saw in Chapter 3 that the spectral content of such signals extends well above the repetition rate of the signal, so that this could cause radiated and/or conducted emission problems.

Both carbon-composition and wire-wound resistors exhibit other nonideal effects. For example, there is a certain "bridging capacitance" from end-to-end due to charge leakage around the resistor body. Usually this is a minor effect. A more significant effect is represented by the *inductance and capacitance of the leads attached to the element*, as was discussed in the previous section. Replacing the leads with a lumped-backward Γ equivalent circuit gives the model shown in Fig. 5.10a. We could have also chosen to use any of the other models of Fig. 5.8, but will choose the lumped-backward Γ model for simplicity. Thus the equivalent circuit of the resistor is as shown in Fig. 5.10b. The lead inductance L_{lead} in this model refers to the inductance of the loop area bounded by the two leads. Values calculated for typical lead lengths of 0.5 in., lead separations of 0.25 in., and lead wires (20-gauge with $r_w = 16$ mils) using (5.5) give L_{lead} of some 14 nH. (The degree of separation is determined largely by the length of the resistor body when the leads are bent at right angles to the body.) The *parasitic* capacitance in this model refers to the parallel combination of the lead and leakage capacitances, $C_{\text{par}} = C_{\text{lead}} + C_{\text{leakage}}$. Typical values are $C_{\text{par}} \cong$ 1–2 pF. Values of C_{lead} calculated for typical lead lengths of 0.5 in., lead separation of 0.25 in., and lead wires (20-gauge with $r_w = 16$ mils) using (5.6) give C_{lead} of some 0.128 pF. This is probably smaller than the leakage capacitance of the resistor

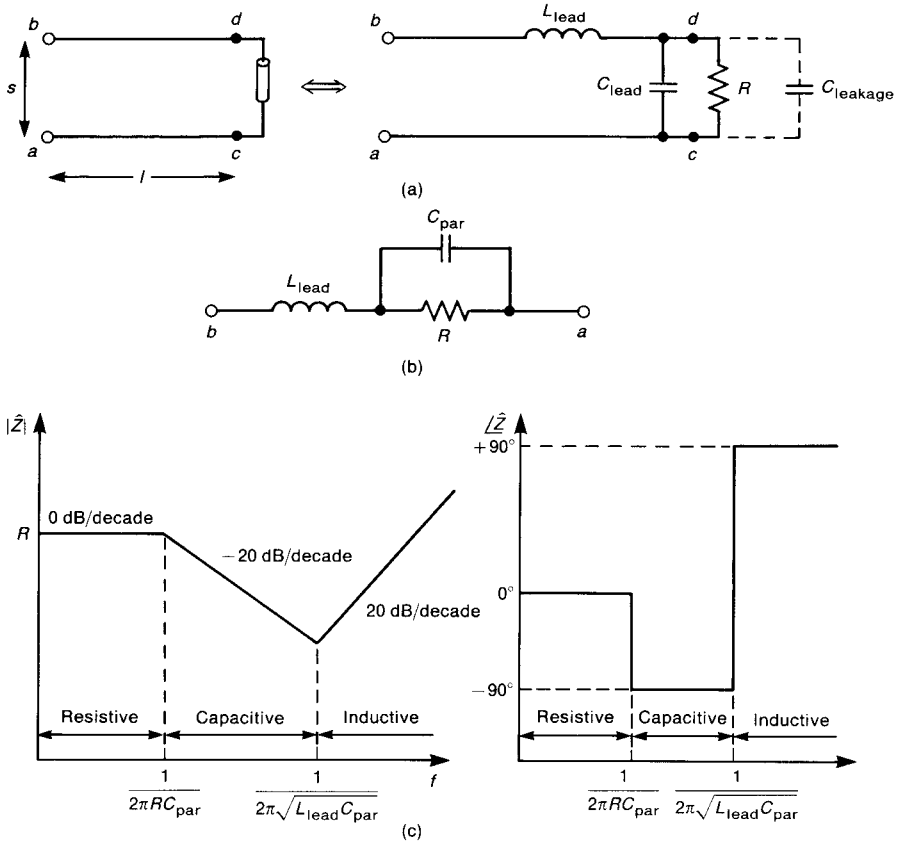

FIGURE 5.10 The nonideal resistor including the effects of the leads: (a) equivalent circuit; (b) simplified equivalent circuit; (c) Bode plots of the impedance variation with frequency.

body. It is instructive to calculate the effect of these elements. Consider a 1-kΩ resistor. If we assume a value of the parasitic capacitance of 1 pF, the impedance of C_{par} is 1 kΩ at a frequency of approximately 159 MHz. The inductance and capacitance resonate at a frequency of approximately 1.3 GHz. This illustrates that for high-impedance resistors the parasitic capacitance is the dominant element effect.

In order to examine the frequency response of this model, we first derive the equation for the impedance of the model. A simple way of doing this is described in [4, 5]. (Also see Appendix A.) First replace the inductors with their impedances in terms of $p = j\omega$ to give $\hat{Z}_L = pL$, and replace the capacitors with their impedance $\hat{Z}_C = 1/pC$. Derive the expression for the impedance of the element $\hat{Z}(p)$, and then substitute $p = j\omega$ in that expression. The impedance $\hat{Z}(p)$ here is a general form of a "transfer function" giving the *ratio* of two circuit quantities (current and/or voltage) [4,5]. The transfer function here is the ratio of the terminal voltage $\hat{V}(p)$

and the terminal current $\hat{I}(p)$ as $\hat{Z}(p) = \hat{V}(p)/\hat{I}(p)$, where the voltage and current are defined with the passive sign convention. For the resistor model of Fig. 5.10b one can derive

$$\hat{Z}(p) = L_{\text{lead}} \frac{p^2 + p/RC_{\text{par}} + 1/L_{\text{lead}}C_{\text{par}}}{p + 1/RC_{\text{par}}} \tag{5.12}$$

Substituting $p = j\omega$ into this expression gives

$$\hat{Z}(j\omega) = L_{\text{lead}} \frac{1/L_{\text{lead}}C_{\text{par}} - \omega^2 + j\omega/RC_{\text{par}}}{j\omega + 1/RC_{\text{par}}} \tag{5.13}$$

The corresponding Bode or asymptotic plot [5] of the magnitude and phase angle of this impedance is given in Fig. 5.10c. We will frequently employ the logarithmic or Bode plot method of displaying the frequency response of elements. The reader should review this method, which is described in any typical circuit analysis text. A complete discussion is given in [5]. The basic method is to plot not the magnitude $|\hat{Z}(j\omega)|$ but the logarithm of the magnitude, $|\hat{Z}(j\omega)|_{\text{dB}} = 20\log_{10}|\hat{Z}(j\omega)|$, in decibels (above or relative to a reference level of $1\,\Omega$). In order that straight lines on the "unlogged" plot translate to straight lines on the log plot, the frequency axis must be plotted as $\log_{10} f$. This is usually more easily accomplished using semilog graph paper where the vertical axis has linear tick mark spacing for plotting $|\hat{Z}(j\omega)|_{\text{dB}} = 20\log_{10}|\hat{Z}(j\omega)|$ and logarithmic spacing of the tick marks on the horizontal axis for plotting the frequency on a logarithmic basis. This is implied when we label the horizontal axes of these plots as simply f. We could also use log–log graph paper with logarithmically spaced tick marks on the vertical axis for plotting the absolute magnitude instead of the magnitude in dB (relative to $1\,\Omega$).

It is important at this point to consider another computational technique. The reader should be able to not only compute the "transfer function" of a circuit but also quickly check the accuracy of the result and determine the gross behavior of the frequency response. In order to do this, we simply check, directly from the circuit, the behavior at two frequencies: dc and infinite frequency. In order to check the behavior at dc, we simply substitute $p = 0$ into any impedance expression. For example, substituting $p = 0$ into $\hat{Z}_L = pL$ and $\hat{Z}_C = 1/pC$ gives

$$\hat{Z}_L = 0|_{f=0} \tag{5.14a}$$

$$\hat{Z}_C = \infty|_{f=0} \tag{5.14b}$$

In other words, an inductor (an ideal one) is a *short circuit* at dc and a capacitor is an *open circuit* at dc. This can be checked directly from the circuit by replacing the inductor with a short circuit and replacing the capacitor with an open circuit. Once this is done, we see that the behavior of the model at dc is the same as an ideal resistor. As we increase the frequency, the impedance of the capacitor decreases and tends to "short out" the resistor of the model. This begins to occur

at a frequency where the impedance of the capacitor equals the resistance, or $\omega_1 = 1/RC_{\text{par}}$. Thus the net impedance decreases at -20 dB/decade and the phase angle approaches -90° above this frequency. At a point where the inductor and capacitor of the model *resonate*, $\omega_0 = 1/\sqrt{L_{\text{lead}}C_{\text{par}}}$, the impedance of the model is at a minimum. (Actually, this minimum occurs at a frequency that is slightly above this resonant frequency, with it approaching this frequency the smaller the value of R.) Above this resonant frequency, the impedance of the inductor becomes dominant and the magnitude of the impedance increases at 20 dB/decade and the phase angle approaches $+90^\circ$. Finally, as the frequency approaches infinity, the inductor behaves as an open circuit and the capacitor behaves as a short circuit, so that the net impedance of the model approaches that of an open circuit (due primarily to the inductor):

$$\hat{Z}_L = \infty|_{f=\infty} \tag{5.15a}$$

$$\hat{Z}_C = 0|_{f=\infty} \tag{5.15b}$$

Since the inductance was dominant for higher frequencies, the phase angle approaches 90°. All of this behavior is borne out by the transfer function that we derived. However, it is always a good idea to perform these simple checks. Also, an understanding of the simple principles described above can be an aid, along with the understanding of the physical construction of the element, in the construction of a suitable model that will represent this nonideal behavior. This examination of the model over distinct frequency ranges is represented in Fig. 5.11. The reader should study this method since it will be used on numerous occasions to examine and construct models of elements and devices.

We will frequently present and examine experimentally obtained data. The purpose in doing so is twofold. First, it is not possible to construct one model that will apply to all frequencies, so we will need to accept some approximate behavior in exchange for model simplicity. A model that will predict the behavior of an element for a very wide frequency range can always be constructed. However, that model will of necessity be very complex, and consequently will yield very little insight into the device behavior. Experimental data will reveal the adequacy of the simpler model. Second, it is important for the reader to obtain some appreciation for the typical range of numerical results. Examining experimental data obtained from actual devices will serve this latter purpose. An example of such data is shown in Fig. 5.12, where the measured impedance of a 1-kΩ, $\frac{1}{8}$-W carbon resistor having 0.5 in. lead lengths and 0.25 in. lead separation is shown over a frequency range of 1–500 MHz. Comparing Fig. 5.12 with Fig. 5.10c, we see that the first breakpoint f_1 occurs at approximately 120 MHz, but the resonant frequency of the model, f_0, is somewhat above the highest measured frequency of 500 MHz. Nevertheless, the model of Fig. 5.10b gives an adequate description of the resistor if we choose $R = 1.05$ kΩ, $C_{\text{par}} = 1.2$ pF, and $L_{\text{lead}} = 14$ nH.

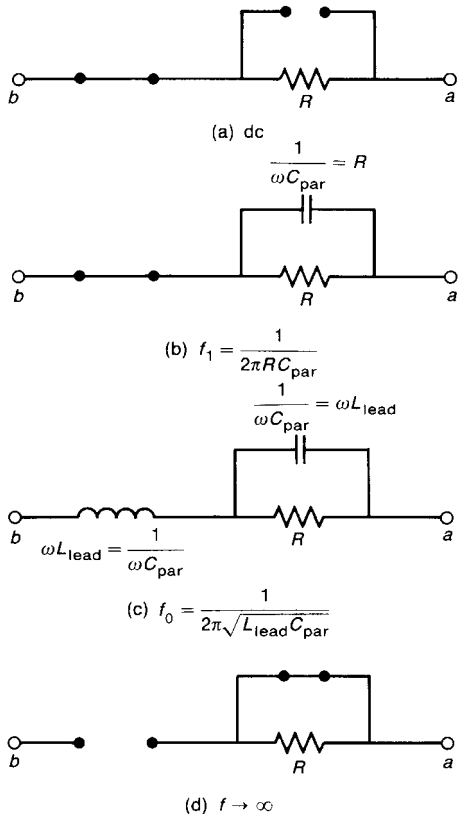

FIGURE 5.11 Simplification of the equivalent circuit of a resistor for various frequencies: (a) dc; (b) $f_1 = 1/2\pi RC_{\text{par}}$; (c) $f_0 = 1/2\pi\sqrt{L_{\text{lead}}C_{\text{par}}}$; (d) as $f \to \infty$.

Example 5.2 Provide a SPICE (PSPICE) simulation of the frequency response of the input impedance to the 1000-Ω resistor shown in Fig. 5.12 [See [4,5] and Appendix D for a discussion of SPICE (PSPICE).]

***Solution*:** The SPICE (PSPICE) simulation circuit is shown in Fig. 5.13. Since we want to provide a frequency response, we use the .AC function. The input impedance is the ratio of the input voltage to the input current. Hence we apply a $1\angle 0^\circ$A current source and the plot input voltage:

$$\hat{Z}_{\text{in}} = \frac{\hat{V}(1)}{1\angle 0^\circ} = \hat{V}(1)$$

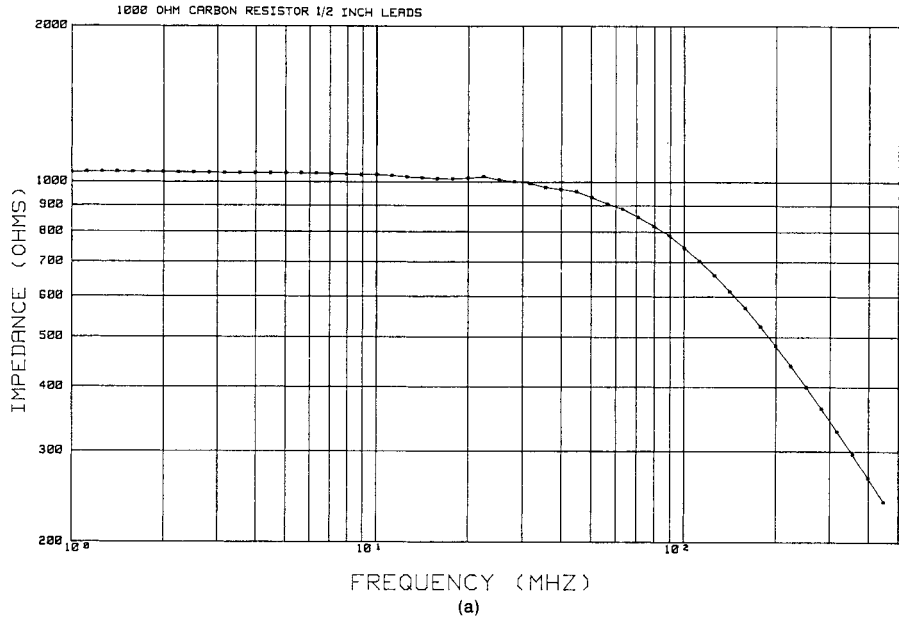

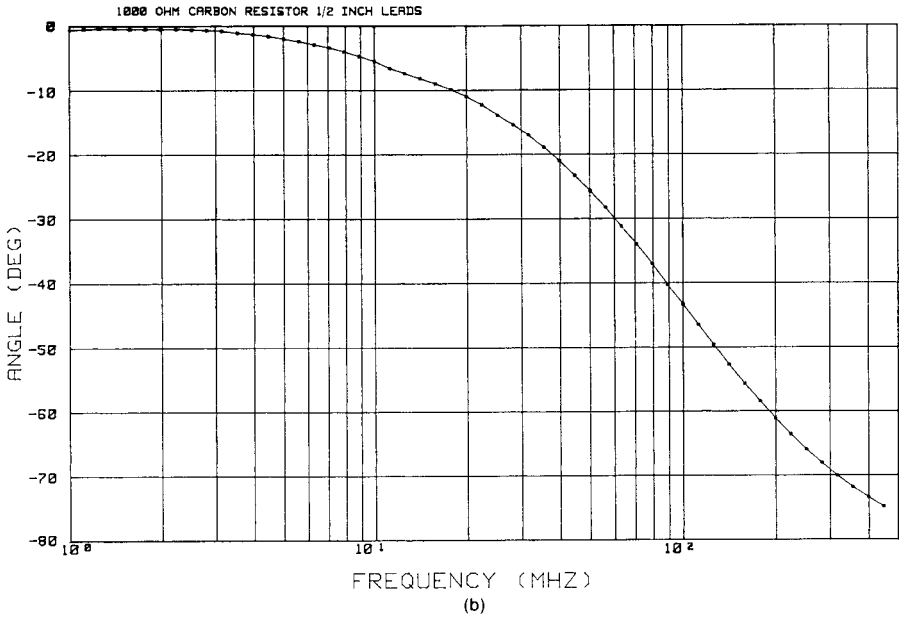

FIGURE 5.12 Measured impedance of a 1000-Ω carbon resistor having $\frac{1}{2}$ in. lead lengths: (a) magnitude; (b) phase.

The PSPICE program is

```
SIMULATION OF 1K OHM CARBON RESISTOR
IS 0 1 AC 1
L 1 2 14NH
C 2 0 1.2PF
R 2 0 1.05K
.AC DEC 50 1MEG 500MEG
.PROBE
END
```

Figure 5.14 shows the plot of the magnitude, VDB(1) and phase VP(1), which match those of Fig. 5.12 rather well.

5.5 CAPACITORS

The ideal behavior of a capacitor is shown in Fig. 5.15. The impedance is $\hat{Z}(p) = 1/pC$, or, by substituting $p = j\omega$, we obtain

$$\begin{aligned}\hat{Z}(j\omega) &= \frac{1}{j\omega C} \\ &= -j\frac{1}{\omega C} \\ &= \frac{1}{\omega C}\underline{/-90^\circ}\end{aligned} \tag{5.16}$$

The magnitude of the impedance decreases linearly with frequency, or -20 dB/ decade, and the phase angle is constant at -90°.

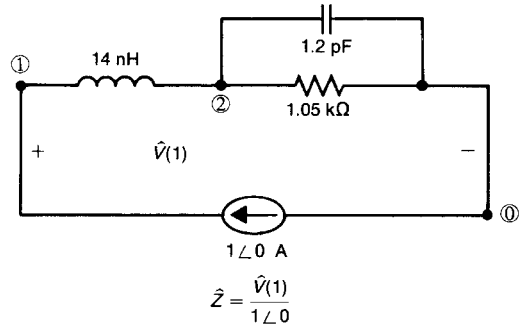

FIGURE 5.13 The SPICE simulation circuit for the 1000-Ω resistor having $\frac{1}{2}$ in. lead lengths.

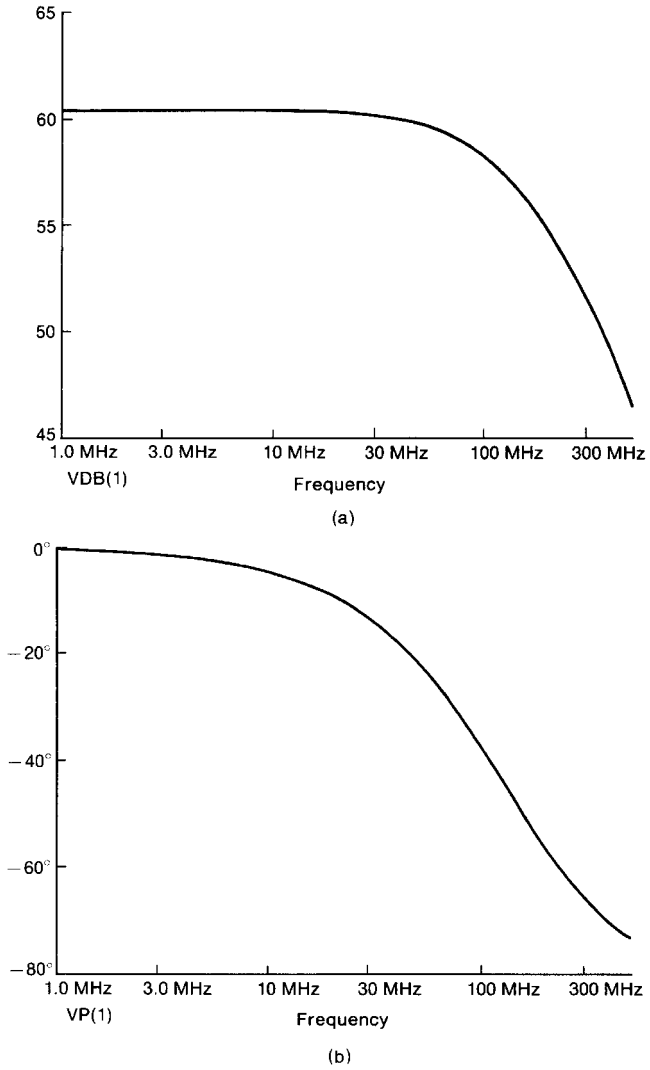

FIGURE 5.14 SPICE predictions of the impedance of a 1000-Ω resistor having $\frac{1}{2}$ in. lead lengths: (a) magnitude; (b) phase.

There are numerous types of capacitors. For the purposes of EMC suppression, the typical types are ceramic and tantalum electrolytic. Large values of capacitance (1–1000 μF) can be obtained in a small package with the tantalum electrolytic capacitor. Ceramic capacitors give smaller values of capacitance (1 μF−5 pF) than do electrolytic capacitors, yet they tend to maintain their ideal behavior up to a much higher frequency. Thus ceramic capacitors are typically used for suppression in the radiated emission frequency range, whereas electrolytic capacitors, by

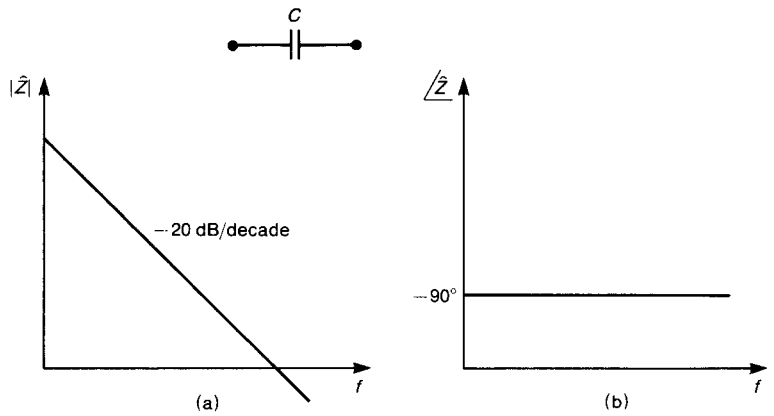

FIGURE 5.15 Frequency response of the impedance of an ideal capacitor: (a) magnitude; (b) phase.

virtue of their much larger values, are typically used for suppression in the conducted emission band and also for providing bulk charge storage on printed circuit boards as we will see. For a more complete discussion of capacitor types see [6].

Both types of capacitors have similar equivalent circuits, but the model element values differ substantially. This accounts for their different behavior over different frequency bands. Both types of capacitor can be viewed as a pair of parallel plates separated by a dielectric, as illustrated in Fig. 5.16. The loss (polarization and ohmic) in the dielectric is represented as a parallel resistance R_{diel} [1]. Usually this is a large value, as one would expect (hope). The resistance of the plates is represented by R_{plate}. For small ceramic capacitors, this is usually small enough in relation to the other elements to be neglected. Once again, the leads

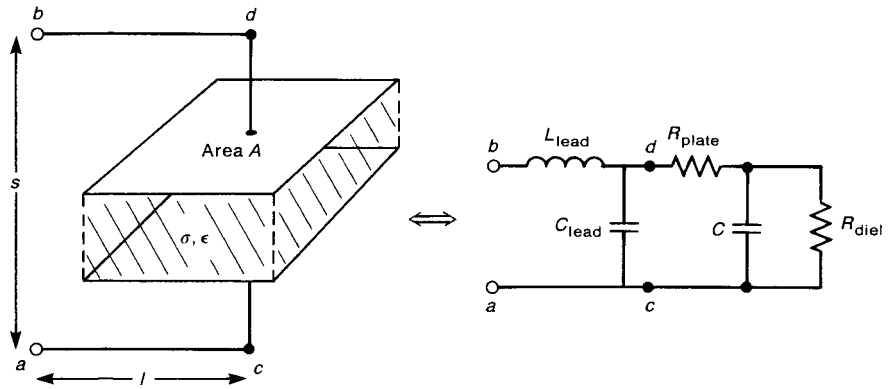

FIGURE 5.16 Modeling of a physical capacitor with an equivalent circuit.

attached to the capacitor have a certain inductance represented by L_{lead} and capacitance C_{lead}. Again, these parasitic element values depend on the configuration of the two leads. If the leads are formed in the shape of a U or bent 90° to the body of the capacitor as is the usual custom then these parasitic lead components are as calculated previously. Usually R_{diel} is so large that it can be neglected. Similarly C_{lead} is usually much less than the ideal capacitance C, and thus may be neglected. Thus the equivalent circuit of the capacitor alone consists of the series combination of C and R_{plate}. The resistance R_{plate} is referred to as the equivalent series resistance or ESR and denoted as R_s. Thus the model consists of the series combination of C, L_{lead}, and R_s, as shown in Fig. 5.17. The ESR is typically several ohms for electrolytic capacitors and varies with frequency. For ceramic capacitors over the regulatory limit frequency range the series resistance is usually negligible. The impedance of this model is

$$\hat{Z}(p) = L_{\text{lead}} \frac{p^2 + R_s p/L_{\text{lead}} + 1/L_{\text{lead}}C}{p} \tag{5.17}$$

Substituting $p = j\omega$ gives

$$\hat{Z}(j\omega) = L_{\text{lead}} \frac{1/L_{\text{lead}}C - \omega^2 + j\omega R_s/L_{\text{lead}}}{j\omega} \tag{5.18}$$

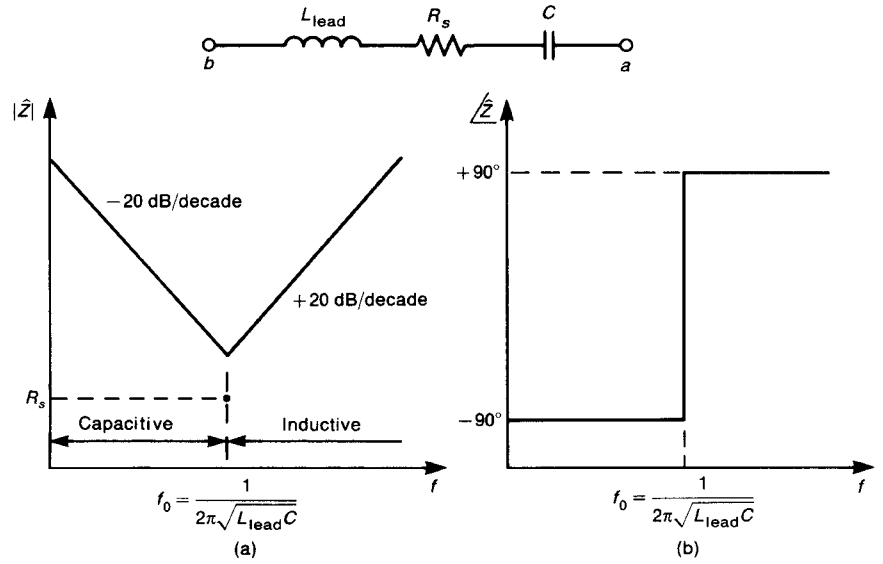

FIGURE 5.17 A simplified equivalent circuit of a capacitor including the effects of lead length showing Bode plots of the impedance: (a) magnitude; (b) phase.

The Bode plots of this impedance are shown in Fig. 5.17. At dc the circuit appears as an open circuit (replace the inductor with a short circuit and the capacitor with an open circuit). As frequency increases, the impedance of the capacitor dominates and decreases linearly with frequency at a rate of -20 dB/decade. The impedance of the inductor increases until it equals that of the capacitor at $f_0 = 1/2\pi\sqrt{L_{\text{lead}}C}$. At this frequency the series combination appears as a short circuit (although the magnitudes of the impedances are equal they are of opposite sign) and the net impedance of the branch is R_s. The frequency f_0 is referred to as the *self-resonant frequency of the capacitor*. For higher frequencies the magnitude of the impedance of the inductor dominates and the impedance increases at a rate of $+20$ dB/decade, while the phase angle approaches $+90^\circ$. If one is relying on this element to provide a low impedance such as for shunting noise currents to ground then the frequency of the current to be suppressed must be lower than the *self-resonant frequency* f_0 of the capacitor or else the impedance will be larger than anticipated on the basis of the ideal behavior of the capacitor.

As an example, suppose the leads of a capacitor are formed into a U shape with a separation of 0.25 in. and length 0.5 in. We calculated previously that the inductance of the loop formed by these leads is $L_{\text{lead}} \cong 14$ nH. Therefore a 470-pF capacitor will resonate at a frequency of 62 MHz and 0.1-μF capacitor will resonate at a frequency of 4.25 MHz. This points out the important fact that, *for a fixed lead length and spacing, the larger the capacitance value the lower the self-resonant frequency* (by the square root of the capacitance ratios). Figures 5.18 and 5.19 show measured impedances of a 470-pF ceramic capacitor from 1 to 500 MHz. Two lead lengths are shown: essentially no lead lengths (Fig. 5.18) and $\frac{1}{2}$ in. lead lengths (Fig. 5.19). Note that the self-resonant frequency for the $\frac{1}{2}$ in. lead length is about 62 MHz, as calculated above. Thus, if one is interested in providing a low impedance to shunt a 200-MHz signal, the 470-pF capacitor with either lead length will give an impedance larger than expected. A 0.15-μF tantalum capacitor was measured, and results are shown from 1 to 500 MHz for essentially no lead lengths and for $\frac{1}{2}$ in. lead lengths in Fig. 5.20 and 5.21, respectively. Note that the frequency response of the tantalum capacitor is not as ideal as that of the ceramic capacitor. This is due to the more significant ESR of the tantalum capacitor.

Review Exercise 5.4 Determine the lead inductance for the 0.15-μF tantalum capacitor having $\frac{1}{2}$ in. lead lengths directly from the measured impedance magnitude in Fig. 5.21a.

***Answer*:** Impedance at 100 MHz is 10 Ω and inductive, giving 15.9 nH.

A frequent mistake made in suppression is in the choice and effectiveness of capacitors [7]. Capacitors are generally the common choice for suppression element since they are easily installable after the product is constructed—simply solder them across the two terminals in a connector or on a PCB to provide a low-impedance path to divert the noise current. Suppose that it is desired to

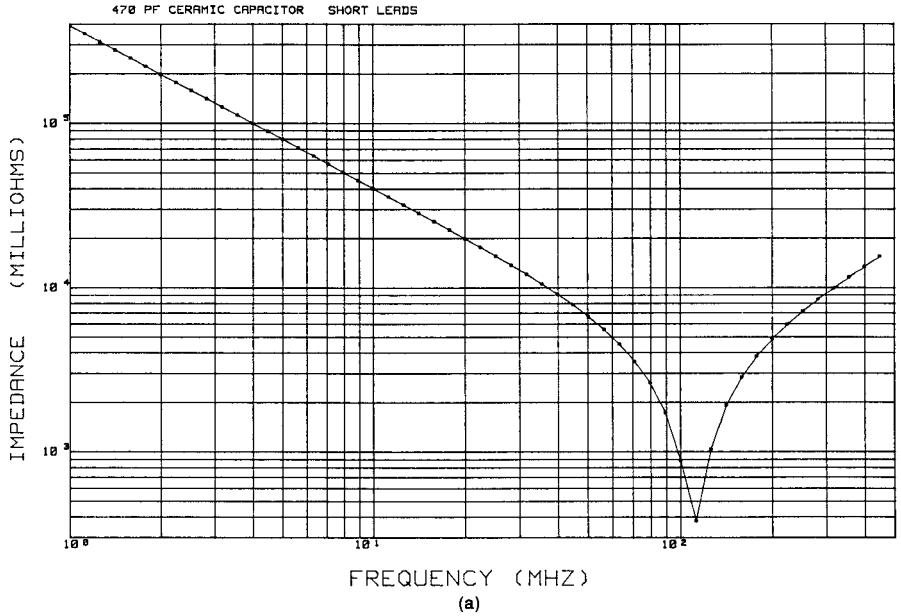

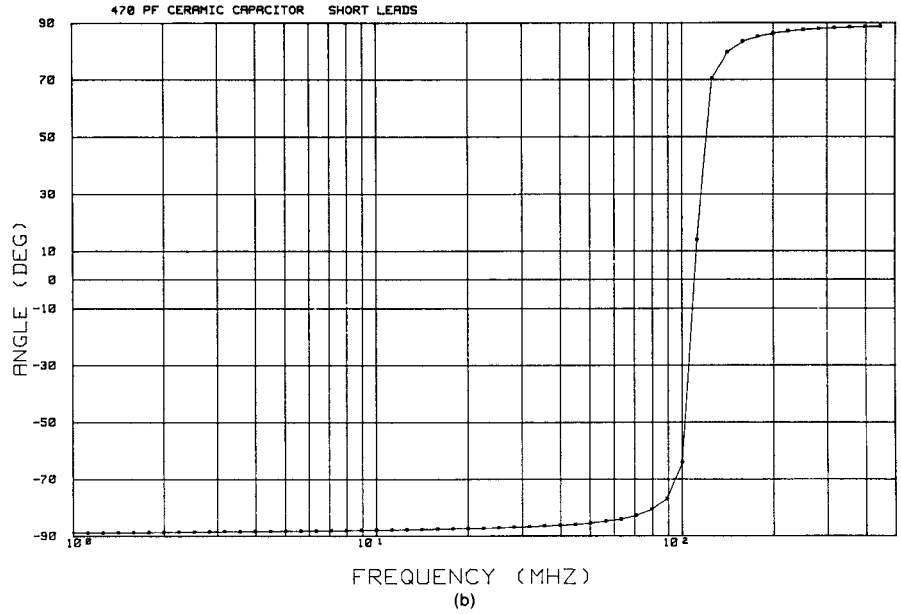

FIGURE 5.18 Measured impedance of a 470-pF ceramic capacitor with short lead lengths: (a) magnitude; (b) phase.

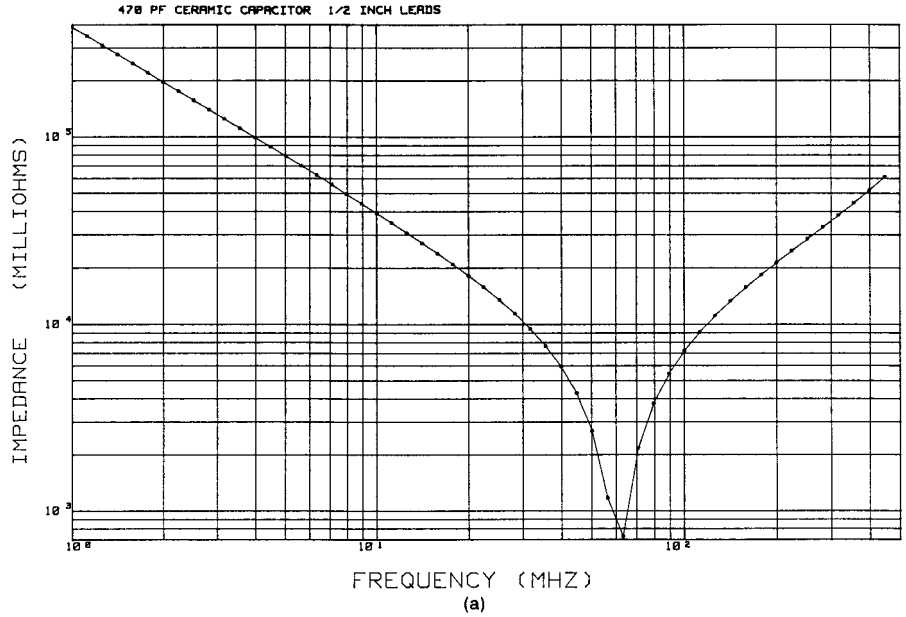

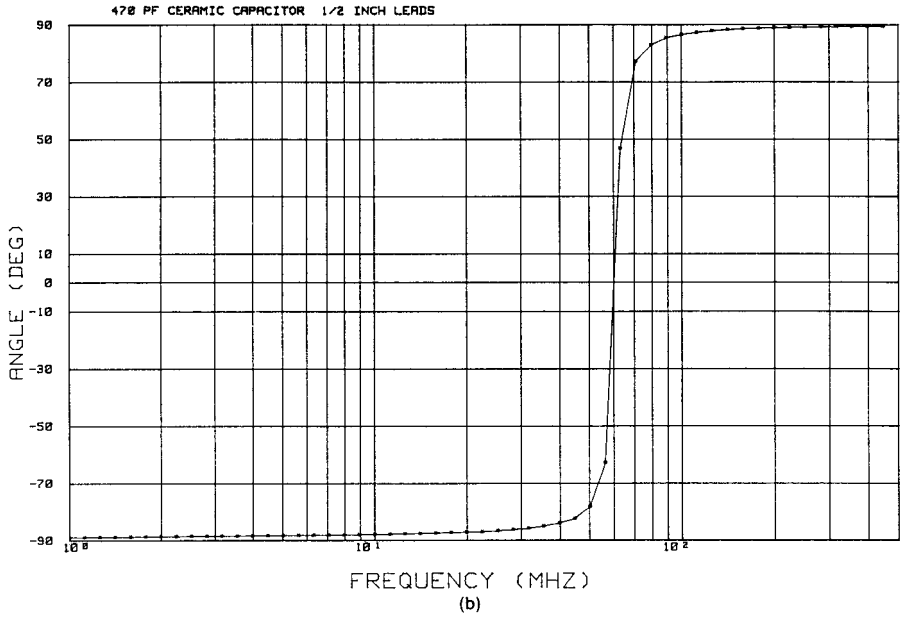

FIGURE 5.19 Measured impedance of a 470-pF ceramic capacitor with $\frac{1}{2}$ in. lead lengths: (a) magnitude; (b) phase.

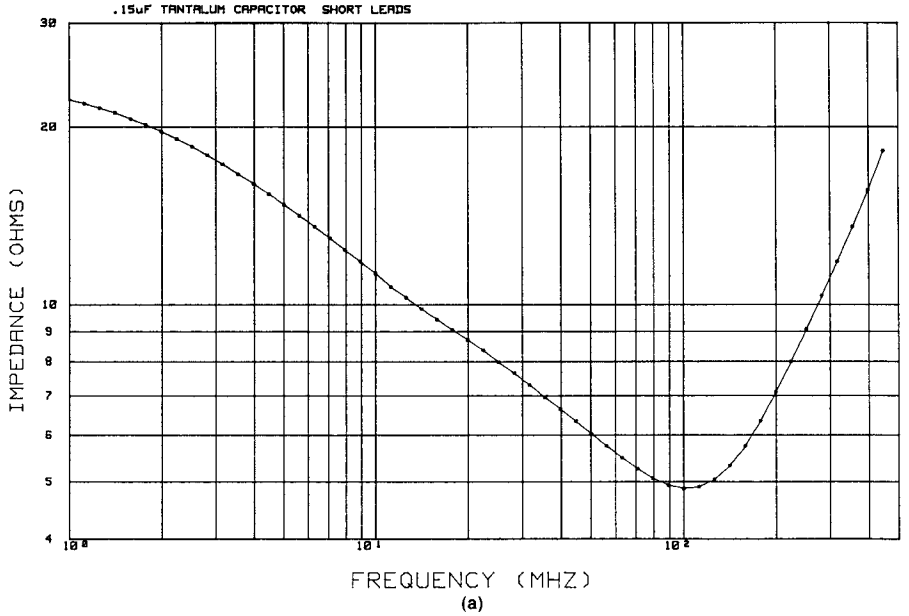

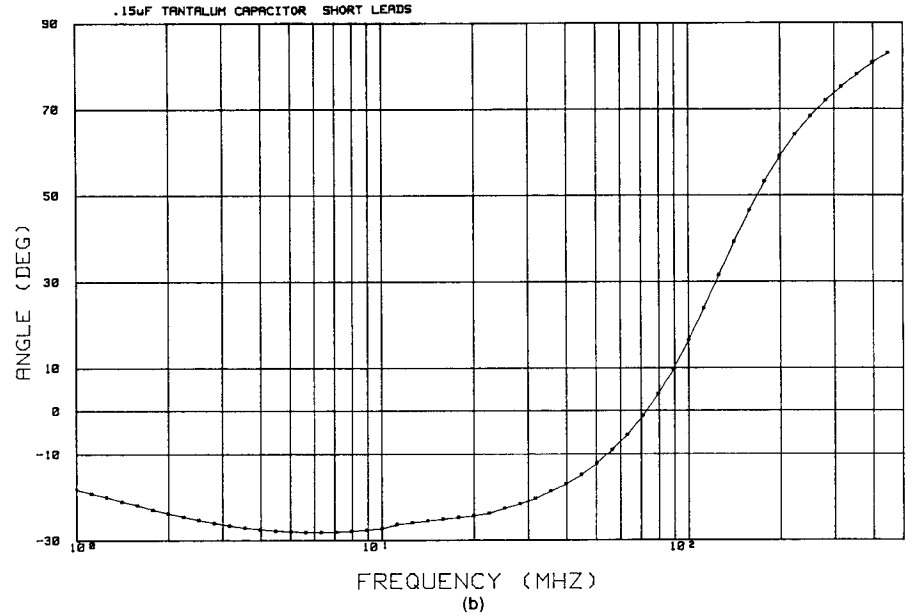

FIGURE 5.20 Measured impedance of a 0.15-μF tantalum capacitor with short lead lengths: (a) magnitude; (b) phase.

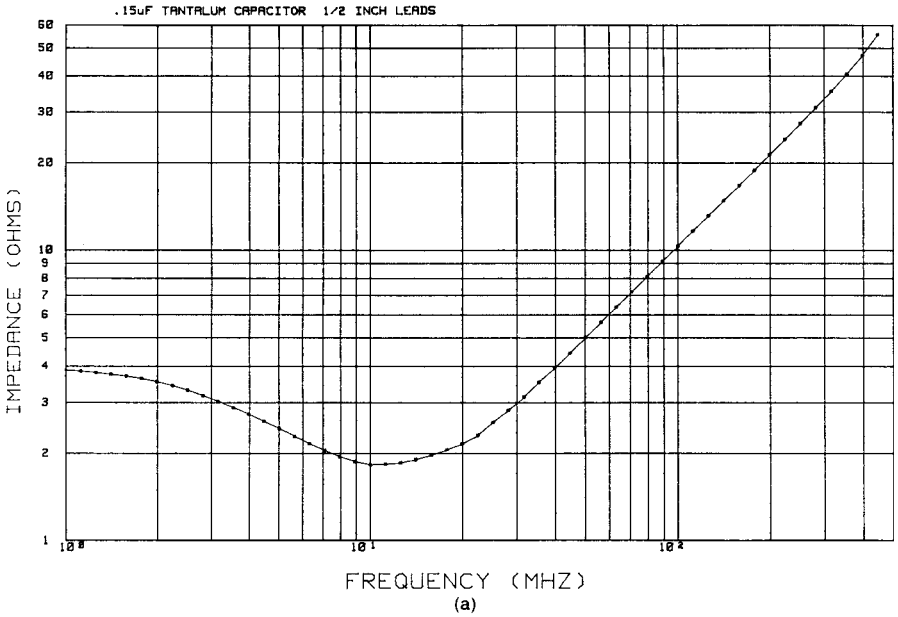

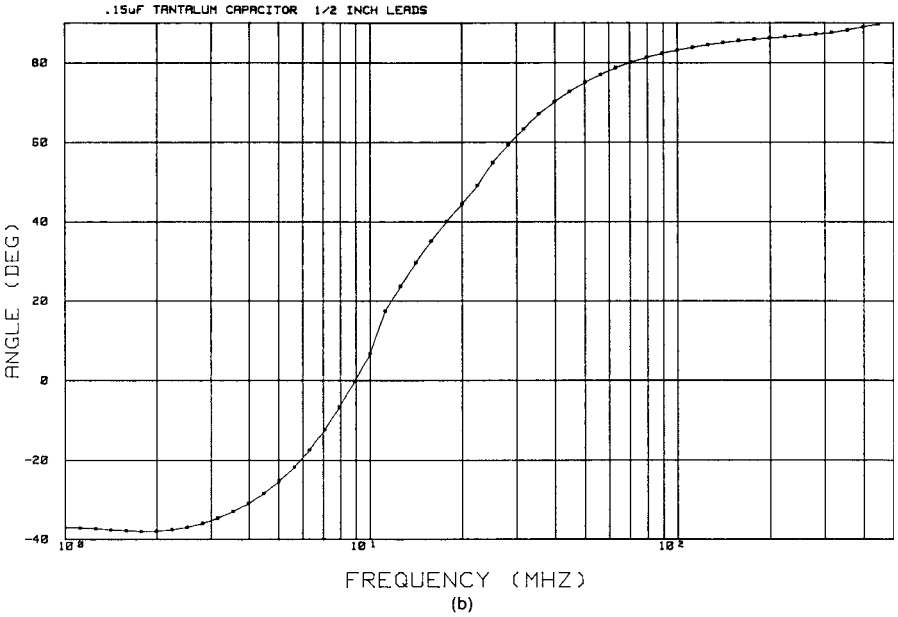

FIGURE 5.21 Measured impedance of a 0.15-μF tantalum capacitor with $\frac{1}{2}$ in. lead lengths: (a) magnitude; (b) phase.

reduce the radiated emission at, say, 100 MHz. Also suppose it is found that the noise current present on a particular peripheral cable is the primary radiation source point. One might place a capacitor between the signal and return wires of the cable where it exits the product in order to divert the high-frequency noise current and prevent it from being present on the pheripheral cable, where its radiation efficiency will be considerably greater. One might choose a ceramic capacitor of value 100 pF. Suppose that the product's radiated emissions are remeasured and found to be reduced, yet this reduction is still not sufficient for the product to comply with the regulatory limit at this frequency. In order to reduce the emission still further, one might be tempted to increase the value of capacitance to, say, 10,000 pF (0.01 μF). When this capacitor is substituted, it will be found that, instead of the radiated emission being reduced (by the expected 40 dB), they are actually increased! What has happened is that the self-resonant frequency of the larger capacitor has been reduced from that of the smaller capacitor not because of any change in L_{lead} but simply because of the larger value of C. Since the self-resonant frequency of the 10,000-pF capacitor is now below the frequency of interest (100 MHz), the capacitor appears inductive, giving an impedance larger than expected. Measured data for 100-pF and 10,000-pF ceramic capacitors, both having 0.5 in. lead lengths, show that the impedance of the 100-pF capacitor at 100 MHz is 8 Ω, whereas the 10,000-pF capacitor has an impedance of 12 Ω at this frequency!

Review Exercise 5.5 Determine the impedance magnitude and phase of a 10,000-pF ceramic capacitor having attachment leads of 20-gauge wire of length 0.5 in. and separation of 0.25 in. at 50 MHz.

***Answer*:** $4.08\underline{/90^\circ}\ \Omega$.

Another caution that should be observed is the effect of the added suppression element on the *functional signals.* Placing a capacitor across the signal and return leads of a cable in order to divert high-frequency signal components from the cable can produce *ringing* by virtue of the resonance created by the capacitor in parallel with the inductance of the cable. Resistors are also frequently inserted in series with the cable in order to block these high-frequency signals. This is frequently implemented by inserting "*RC* packs" in the PCB to provide a low pass filter, where the offboard cable connector exits the PCB. The values of R and C in the implementation described above should be chosen carefully. Suppose that the input to this circuit is a trapezoidal pulse train representing a typical digital signal such as digital data that are being transmitted over the peripheral cable into which the *RC* circuit has been inserted. For the present we will ignore the effect of the peripheral cable. The transfer function of the *RC* circuit so formed is flat out to the break frequency of $1/2\pi RC$ and decreases at a rate of -20 dB/decade above that. Thus we have formed a *lowpass filter.* If the break frequency occurs low enough in the frequency range in comparison with the spectrum

of the signal to be passed by the cable due to large values of R or C, the waveform of the signal can be adversely affected, resulting in functional performance problems. On the other hand, if these values are too small, very little filtering of the high-frequency noise on the cable may occur. (See Fig. 3.27 of Chapter 3, which illustrates this.) This indicates two important points: (1) one must be careful to not adversely affect the functional signal with a suppression scheme, or else passing the regulatory limits will be a moot point: and (2) if the added suppression scheme does not produce a sufficient reduction, one should not be confused, since there is a reason why it does not.

It is also important to understand the concept illustrated in Fig. 5.22. Suppose that a capacitor is to be placed in parallel with a cable or a pair of lands on a PCB in order to divert a noise current $\hat{I}_{\text{NOISE}}$. The impedance of the capacitor is represented by $\hat{Z}_{\text{CAP}}$, and the impedance seen looking into the pair of conductors that we wish to divert the noise current from is designated by $\hat{Z}_{\text{LOAD}}$. By current division, the portion of the noise current that is diverted through the capacitor is given by [4,5]

$$\hat{I}_C = \frac{\hat{Z}_{\text{LOAD}}}{\hat{Z}_{\text{CAP}} + \hat{Z}_{\text{LOAD}}} \hat{I}_{\text{NOISE}} \tag{5.19}$$

If $\hat{Z}_{\text{LOAD}}$ is *large* compared with $\hat{Z}_{\text{CAP}}$, then the capacitor will be effective in keeping $\hat{I}_{\text{NOISE}}$ off the cable. On the other hand, if $\hat{Z}_{\text{LOAD}}$ is *small* compared with $\hat{Z}_{\text{CAP}}$, then the capacitor will be ineffective in diverting noise current! This is why the use of parallel capacitors in *low-impedance* circuits is usually *ineffectual.* They are most effective with *high-impedance* loads. *Whenever a parallel suppression component is to be used, the impedance levels of not only the element but also the parallel path should be computed or estimated at the desired frequency. If* $\hat{Z}_{\text{LOAD}} \ll \hat{Z}_{\text{CAP}}$, *then the suppression component will be ineffectual.* Therefore it is important to remember that *parallel capacitors work best in high-impedance circuits* with regard to diverting noise currents.

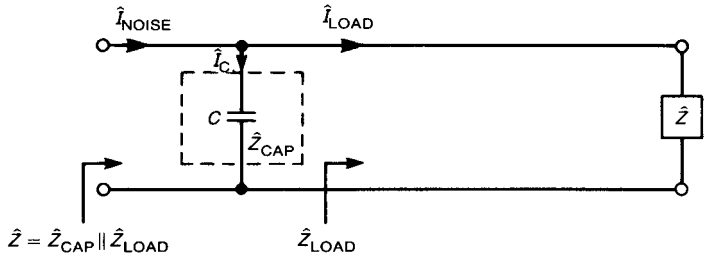

FIGURE 5.22 An important consideration in the diversion of currents with a parallel element: current division and the impedance of the load.

Review Exercise 5.6 A capacitor is placed in parallel with a 1000-Ω resistive load as shown in Fig. 5.22. Determine the value of capacitor such that 90% of a 100 MHz current is diverted through it. (Use the current division principle.)

***Answer*:** 3.3 pF.

5.6 INDUCTORS

The impedance of an ideal inductor is plotted against frequency in Fig. 5.23, and is given by

$$\begin{aligned}\hat{Z}_L &= j\omega L \\ &= \omega L \angle 90^\circ\end{aligned} \tag{5.20}$$

The magnitude increases linearly with frequency at a rate of +20 dB/decade, and the angle is +90° for all frequencies.

There are numerous variations of the basic construction technique of winding turns of wire on a cylindrical form. The specific construction technique will determine the values of the *parasitic* elements in the model of the nonideal inductor that is shown in Fig. 5.24. The process of winding turns of wire on a cylindrical form introduces resistance of the wire as well as capacitance between neighboring turns. This produces the parasitic elements R_{par} and C_{par} in the nonideal model. Some construction techniques wind the turns of wire in *layers* to shorten the length of the inductor body. But this adds capacitance between layers, which *substantially increases* C_{par}. The nonideal inductor should also include the inductance

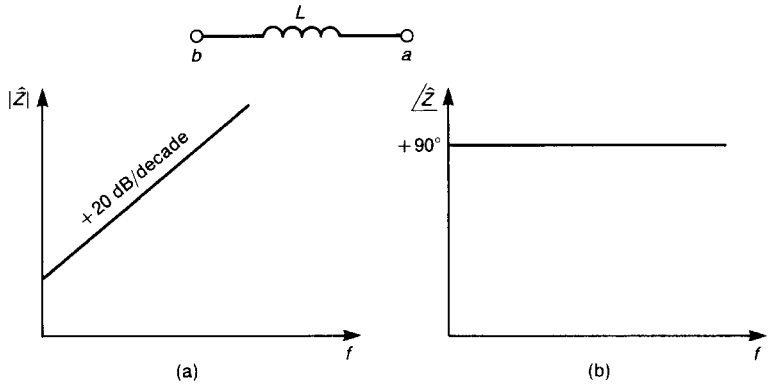

FIGURE 5.23 Frequency response of the impedance of an ideal inductor: (a) magnitude; (b) phase.

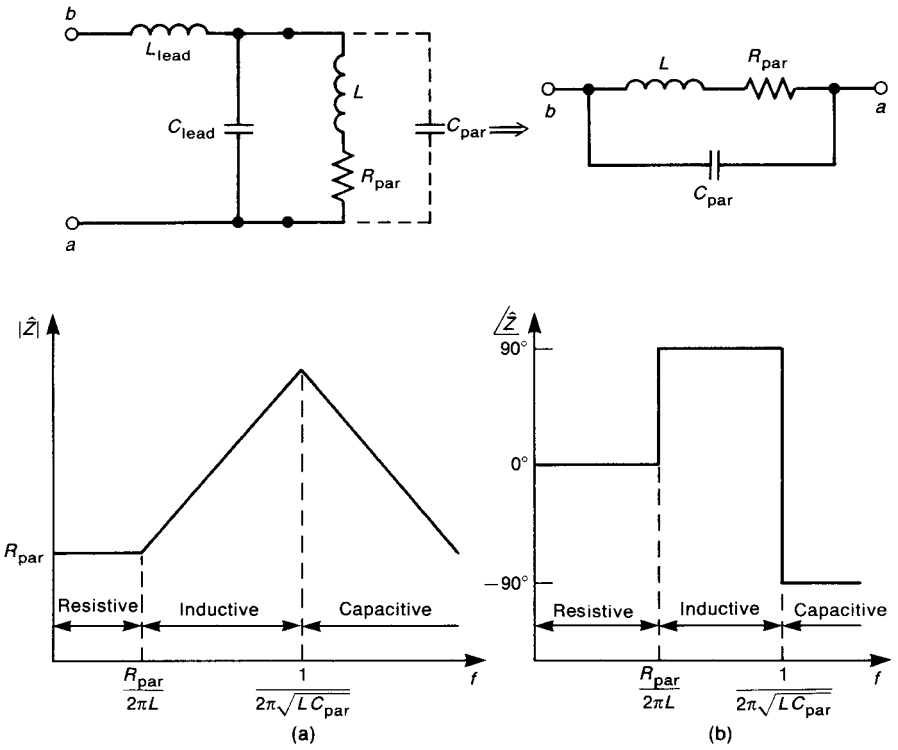

FIGURE 5.24 A simplified equivalent circuit of an inductor including the effects of lead inductance and capacitance showing Bode plots of the impedance: (a) magnitude; (b) phase.

of the attachment leads L_{lead}, as with all other elements. However since the *intentional element* is an inductance and its value is usually much larger than the lead inductance, we may generally neglect L_{lead} in this nonideal model. Similarly, the lead capacitance C_{lead} is frequently less than the parasitic capacitance C_{par}, so that we may neglect the lead capacitance. Thus the model consists of the series combination of R_{par} and L in parallel with C_{par}. The impedance of this model becomes

$$\hat{Z}_L(p) = R_{\text{par}} \frac{1 + pL/R_{\text{par}}}{p^2 LC_{\text{par}} + pR_{\text{par}}C_{\text{par}} + 1} \tag{5.21}$$

Substituting $p = j\omega$ gives

$$\hat{Z}_L(j\omega) = R_{\text{par}} \frac{1 + j\omega L/R_{\text{par}}}{1 - \omega^2 LC_{\text{par}} + j\omega R_{\text{par}}C_{\text{par}}} \tag{5.22}$$

At low frequencies the resistance dominates, and the impedance is R_{par}. As frequency is increased, the inductance of the model begins to dominate at a frequency of $\omega = R_{\text{par}}/L$, and the impedance increases at 20 dB/decade while the angle is $+90^\circ$. As frequency is further increased, the impedance of the parasitic capacitance decreases until its magnitude equals that of the inductor impedance. This occurs at the *self-resonant frequency* of the inductor, $f_0 = 1/2\pi\sqrt{LC_{\text{par}}}$. The Bode plot of the model is also shown in Fig. 5.24.

The measured impedance of a 1.2-μH inductor is shown in Fig. 5.25 from 1 to 500 MHz. The self-resonant frequency of this inductor is of order 110 MHz. This gives a value of C_{par} of 1.7 pF. The measured impedance of a 10-μH inductor gives a value of parasitic capacitance 1.6 pF and a self-resonant frequency of around 40 MHz. This result is reasonable to expect, since the resonant frequency should be reduced by the square root of the ratio of the inductances if the lead lengths and parasitic capacitances are the same. Once again, it is important to remember that *increasing the value of an inductor will not necessarily give a lower impedance at high frequencies, since the larger value of inductance will serve to lower the self-resonant frequency, even though the lead lengths remain identical.*

Review Exercise 5.7 Determine the value of the inductance in the measured data of Fig. 5.25a directly from the data.

***Answer*:** At 4 MHz the impedance is approximately 30 Ω, giving the value of inductance of 1.2 μH.

Capacitors are used to *divert* noise currents, whereas inductors are placed in series with wires or lands to *block* noise currents. This will be effective *if the impedance of the inductor at the frequency of the noise current is larger than the original series impedance seen looking into the wires or lands*, $\hat{Z}_{\text{LOAD}}$, as shown in Fig. 5.26. The choice of whether to use a parallel capacitor to divert noise currents or a series inductor to block noice currents depends strongly on the impedance that it is placed in series or parallel with. *If* $\hat{Z}_{\text{LOAD}}$ *is large, then a rather large value of inductance will be required in order to increase the net impedance of the circuit and provide any blockage of the noise current*! This is why *series inductors are most effective in low-impedance circuits.* Conversely, parallel capacitors must present a much smaller impedance than $\hat{Z}_{\text{LOAD}}$ in order to divert noise currents, so that *parallel capacitors are most effective in high-impedance circuits.*

As with parallel suppression capacitors, one must be concerned with the effect of the suppression element on the functional signal. Addition of series inductors can cause ringing, which can affect the desired performance of the system. However, they are quite effective in lines that do not carry high-speed signals and operate infrequently, such as reset lines of digital devices and the green wire of power cords.

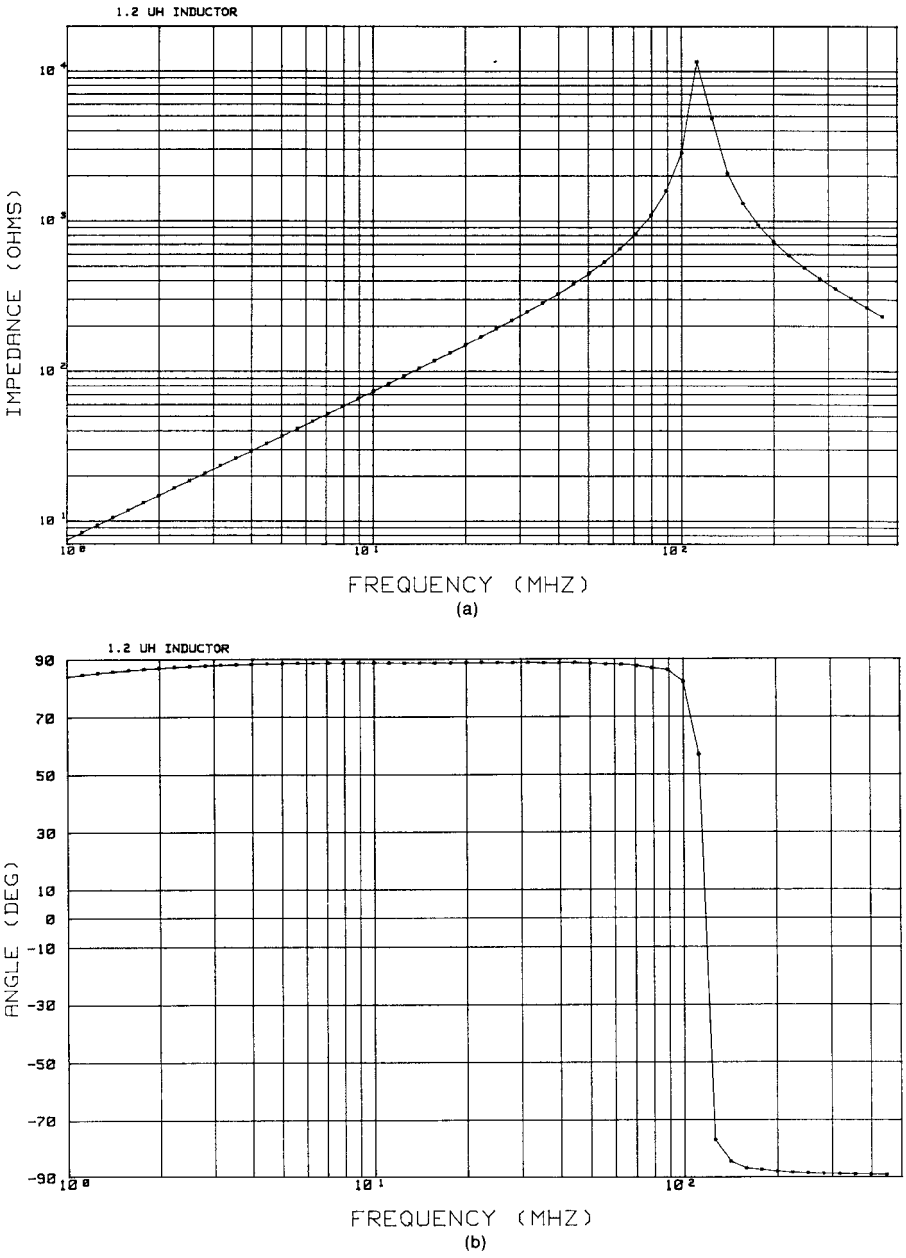

FIGURE 5.25 Measured impedance of a 1.2-μH inductor: (a) magnitude; (b) phase.

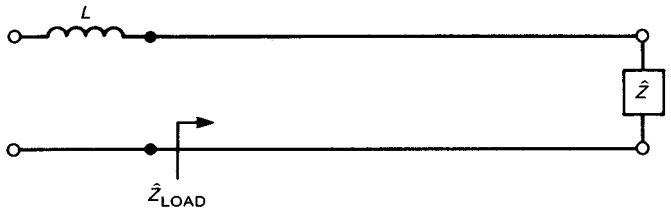

FIGURE 5.26 An important consideration in the blocking of currents with a series element: the impedance of the load.

5.7 FERROMAGNETIC MATERIALS—SATURATION AND FREQUENCY RESPONSE

Ferromagnetic materials are widely used in EMC for noise suppression. All ferromagnetic materials have certain properties that are important to recognize when applying them in EMC applications. The three most important ones are (1) saturation, (2) frequency response, and (3) the ability to concentrate magnetic flux. Consider the toroid inductor shown in Fig. 5.27a. In order to increase the value of inductance of an inductor, inductors are wound on a *ferromagnetic core.* There are numerous types of these ranging from iron to powdered ferrite materials. All types of ferromagnetic materials have large relative permeabilities μ_r, where the permeability is $\mu = \mu_r\mu_0$. For example, steel (SAE 1045) has a relative permeability of $\mu_r = 1000$ and mumetal has $\mu_r = 30{,}000$. Non-ferromagnetic metals such as copper and aluminum have relative permeabilities of free space, $\mu_r = 1$. The values of relative permeability cited for these materials are values measured at *low currents* and at *low frequencies*, typically 1 kHz or lower. Ferromagnetic materials suffer from the property of *saturation*, illustrated in Fig. 5.27a. Consider a ferromagnetic *toroid* that has N turns of wire wound on it. An approximate value for the inductance of this toroid (assuming that all the magnetic flux is confined to the core) is $L = \mu_r\mu_0 N^2 A/l$, where A is the core cross-sectional area and l is the mean path length of the core [1]. Suppose that a current I is passed through the turns. This current creates a *magnetic field intensity* H that is proportional to the product of the number of turns and the current, NI. A *magnetic flux density* B is produced in the core. The product of B and the cross-sectional area of the core, A, gives the magnetic flux $\psi = BA$, whose units are webers. The relationship between H and B is also shown in Fig. 5.27a. The permeability is the *slope* of this B–H curve:

$$\mu = \frac{\Delta B}{\Delta H} \tag{5.23}$$

At low values of current I the slope of the B–H curve is large, as is the permeability. As current is increased, the *operating point* moves up the curve and

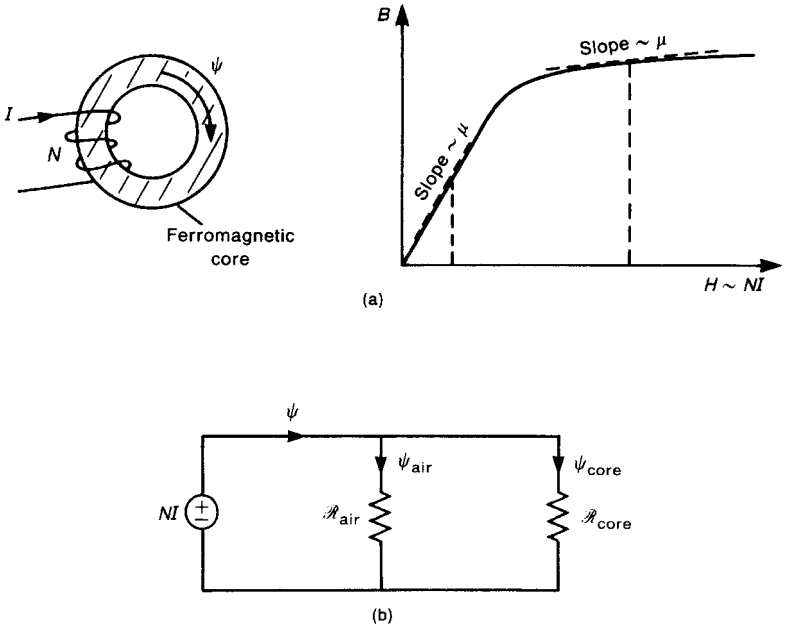

FIGURE 5.27 (a) The nonlinear relationship between magnetic flux density and magnetic field intensity for a ferromagnetic core inductor and (b) an equivalent circuit relating core and air (leakage) fluxes for a ferromagnetic core inductor.

the slope decreases. Thus the *permeability decreases with increasing current.* Since the inductance is a direct function of the permeability of the core, the *inductance decreases with increasing current.* We will have numerous occasions to see this phenomenon in the future. This phenomenon of lowering the relative permeability of a ferromagnetic core with increasing current is referred to as *saturation.*

Ferromagnetic materials have a considerable effect on magnetic fields. *Magnetic fields tend to concentrate in high-permeability materials.* For example, in the ferromagnetic-core inductor shown in Fig. 5.27a we indicated that the magnetic flux ψ was confined to the ferromagnetic core. This is correct to a reasonable approximation. Some of the flux *leaks out* and completes the magnetic path through the surrounding air. The division between how much of the total flux remains in the core and how much leaks out depends on the *reluctance* of the core [1,5]. The quantity of reluctance $\mathscr{R}$ depends on the permeability μ of the magnetic path, its cross-sectional area A, and its length l as [1]

$$\mathscr{R} = \frac{l}{\mu A} \tag{5.24}$$

An important analogy to ordinary lumped circuits can be used to analyze magnetic circuits. It consists of making the analogy of voltage to *magnetomotive force (mmf)*, which is given in ampere turns, *NI*, and current to magnetic flux ψ as

$$R = \frac{NI}{\psi} \tag{5.25}$$

The equivalent circuit for the toroidal inductor of Fig. 5.27a is given in Fig. 5.27b. By current division, the portion of the total flux ψ that remains in the core is

$$\psi_{\text{core}} = \frac{\mathscr{R}_{\text{air}}}{\mathscr{R}_{\text{air}} + \mathscr{R}_{\text{core}}}\psi \tag{5.26}$$

For high-permeability cores, $R_{\text{core}} \ll \mathscr{R}_{\text{air}}$, so that the majority of the flux is confined to the core. The reluctances of the paths are proportional to the permeabilities of the paths, so that the portion of the total flux that remains in the core is proportional to the ratios of the *relative permeabilities* of the two paths. Cores constructed from ferromagnetic materials such as steel, which has $\mu_r = 1000$, tend to have small leakage flux. We will use this notion of *lowering the reluctance of a magnetic path in order to concentrate magnetic flux in that path* on numerous occasions in the future.

It seems that we should select a ferrite core material that has the highest *initial permeability* possible in order to concentrate the flux in the core. Ferrite core materials have different frequency responses of their permeability. A core having an initial relative permeability of 2000 at 1 kHz and low current might have that relative permeability reduced to under 100 at frequencies in the frequency range of the regulatory limit *where it is to have an effect.* Figure 5.28 illustrates this point. Manufacturers of ferrite core materials have their individual mix of materials they use to fabricate the ferrite material. However, ferrites typically are predominantly either of manganese zinc (MnZn) or nickel zinc (NiZn). Manganese zinc ferrites tend to have the high initial permeabilities, *but* their permeabilities deteriorate more rapidly with increasing frequency than do nickel zinc ferrites. Therefore, although a ferrite core having a large initial permeability may seem more attractive than one with a lower value, it should be remembered that in the range of the radiated emission limit (30 MHz–40 GHz) the core having the lower initial permeability may well have the higher permeability of the two, and is therefore preferred for use in suppressing the spectral components of currents in this frequency range. Typical EMC laboratories have specific cores to be used for conducted emission suppression and others to be used for radiated emission suppression because of these considerations.

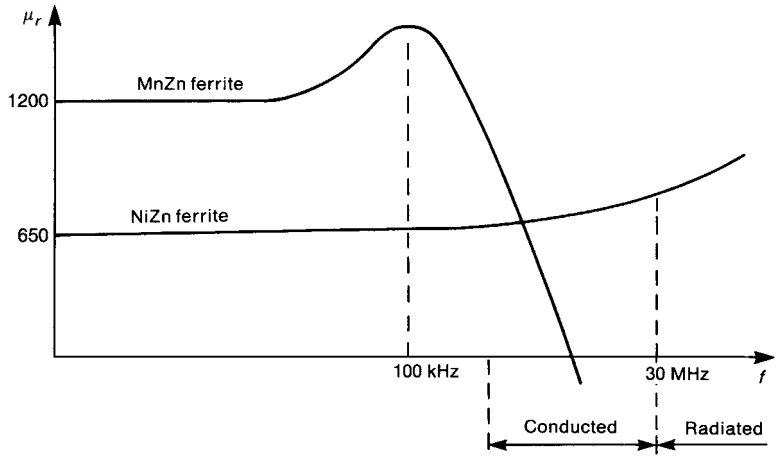

FIGURE 5.28 Frequency response of the relative permeabilities of MnZn and NiZn ferrites.

In order to illustrate this frequency dependence, we have shown the frequency response of the impedance of an inductor formed by winding 5 turns of 20-gauge wire on two toroids in Fig. 5.29. Figure 5.29a shows the impedance for a typical MnZn core, while Fig. 5.29b shows the impedance for a typical NiZn core. Note that the MnZn core shows an impedance of some 500 Ω at 1 MHz, whereas the NiZn core shows an impedance of some 80 Ω at 1 MHz. However, at a frequency of 60 MHz, the MnZn core shows an impedance of 380 Ω, whereas the NiZn core shows an impedance of 1200 Ω! This illustrates that the type of core to be used depends on the frequency of application (suppression of conducted emissions or radiated emissions). Unless one is careful to catalogue the cores in the inventory such as by painting them with different colors, the proper selection can be difficult.

Figure 5.30 shows photographs of various configurations of ferrite cores. These are available to clamp around round cables such as video cables or ribbon and flat-pack cables.

5.8 FERRITE BEADS

Ferrite materials are basically nonconductive ceramic materials that differ from other ferromagnetic materials such as iron in that they have low eddy-current losses at frequencies up to hundreds of megahertz. Thus they can be used to provide selective attenuation of high-frequency signals that we may wish to suppress from the standpoint of EMC and not effect the more important lower-frequency components of the functional signal. These materials are available in various

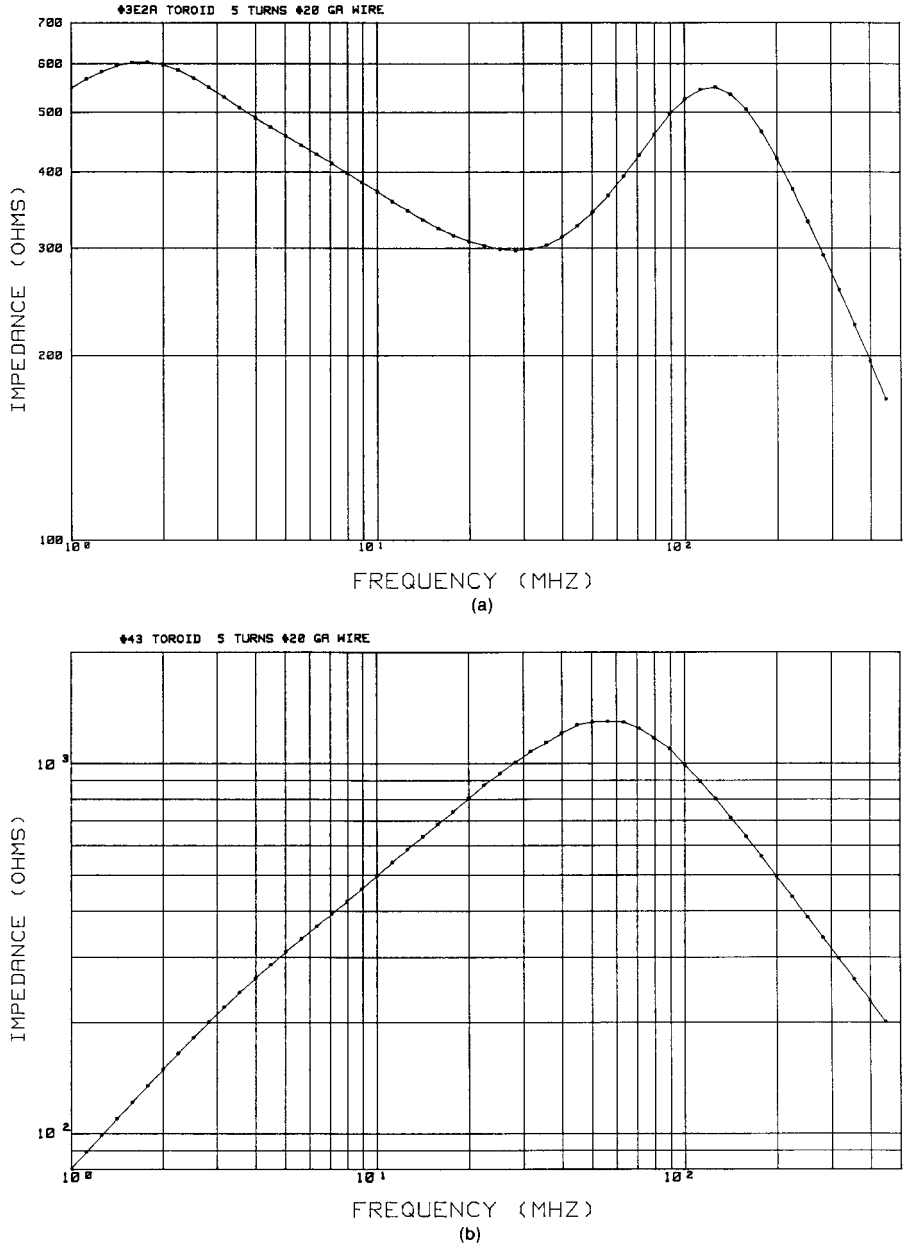

FIGURE 5.29 Measured impedances of inductors formed by winding 5 turns of 28-gauge wire on (a) MnZn and (b) NiZn cores.

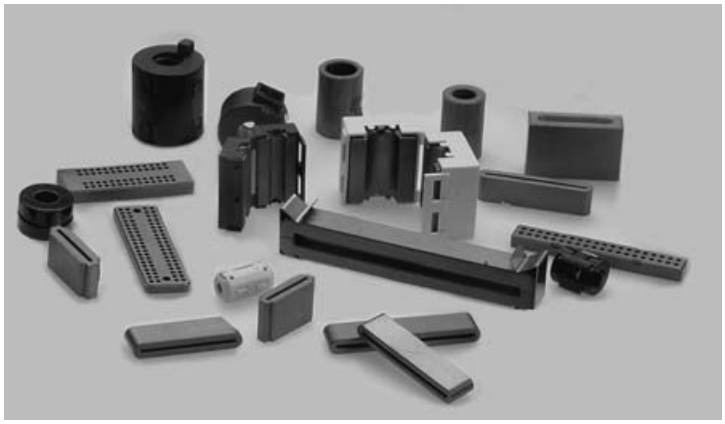

FIGURE 5.30 Photos of various configurations of ferrites for various applications. (Courtesy of G-MAG, Inc.)

forms. The most common form is a *bead* as shown in Fig. 5.31. The ferrite material is formed around a wire, so that the device resembles an ordinary resistor (a black one without bands). It can be inserted in series with a wire or land and provide a high-frequency impedance in that conductor.

The current passing along the wire produces magnetic flux in the circumferential direction, as we observed previously. This flux passes through the bead material, producing an internal inductance in much the same way as for a wire considered in Section 5.1.1. Thus the inductance is proportional to the permeability of the bead material: $L_{\text{bead}} = \mu_0 \mu_r K$, where K is some constant depending on the bead dimensions. The bead material is characterized by a complex relative permeability as

$$\mu_r = \mu_r'(f) - j\mu_r''(f) \tag{5.27}$$

The real part μ_r' is related to the stored magnetic energy in the bead material, while the imaginary part μ_r'' is related to the losses in the bead material. Both are shown as being functions of frequency. Substituting this into the general equation for the

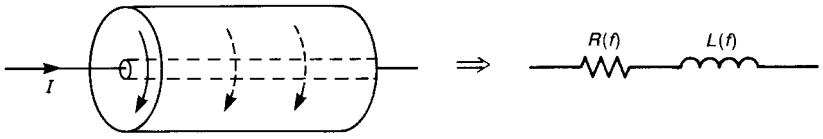

FIGURE 5.31 A ferrite bead.

impedance of the bead inductance gives

$$\begin{aligned} j\omega L_{\text{bead}} &= j\omega\mu_0\mu_r K \\ &= j\omega\mu_0(\mu_r' - j\mu_r'')K \\ &= \underbrace{\omega\mu_r''(f)\mu_0 K}_{R(f)} + \underbrace{j\omega\mu_r'(f)\mu_0 K}_{L(f)} \end{aligned} \tag{5.28}$$

From this result we see that the equivalent circuit consists of a resistance that is dependent on frequency in series with an inductance that is also dependent on frequency. Typical ferrite beads can be expected to give impedances of order 100 Ω above approximately 100 MHz. *Multiple-hole* ferrite beads as illustrated in Fig. 5.32 can be used to increase this high-frequency impedance. The measured impedances of a $\frac{1}{2}$-turn (a bead surrounding a wire) ferrite bead and a $2\frac{1}{2}$-turn ferrite bead from 1 to 500 MHz are shown in Fig. 5.33.

Because the impedance of ferrite beads is limited to several hundred ohms over the frequency range of their effectiveness, they are typically used in *low-impedance* circuits such as power supplies. They are also used to construct lossy filters. For example, placing a ferrite bead in series with a wire and placing a capacitor between the two wires will constitute a two-pole, lowpass filter. A series ferrite bead can also act to damp ringing in fast-rise time circuit. Ferrites are available in other forms. A more recent use has been in the placement of ferrite slabs under dual-in-line (DIP) packages. The ferrite slab has holes drilled along its edges that correspond to the pin spacings of the DIP package. The pins of the DIP are placed through these holes and the combination inserted into a carrier or soldered directly to the PCB. An example of this use to damp very high-frequency oscillations is described in [8].

Ferrite beads are no different than other uses of ferrites in that they are susceptible to saturation when used in circuits that pass high-level, low-frequency currents. A ferrite bead placed in series with the 60 Hz power lead would probably be saturated by this high-level (1–10-A) current.

5.9 COMMON-MODE CHOKES

We now embark on a discussion of one of the most important topics affecting the radiated emissions of products, *common-mode* and *differential-mode currents.* Consider the pair of parallel conductors carrying currents $\hat{I}_1$ and $\hat{I}_2$, as shown in Fig. 5.34. We may *decompose* these two currents into two auxiliary currents, which we refer to

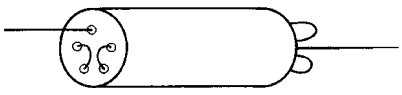

FIGURE 5.32 A multiturn ferrite bead.

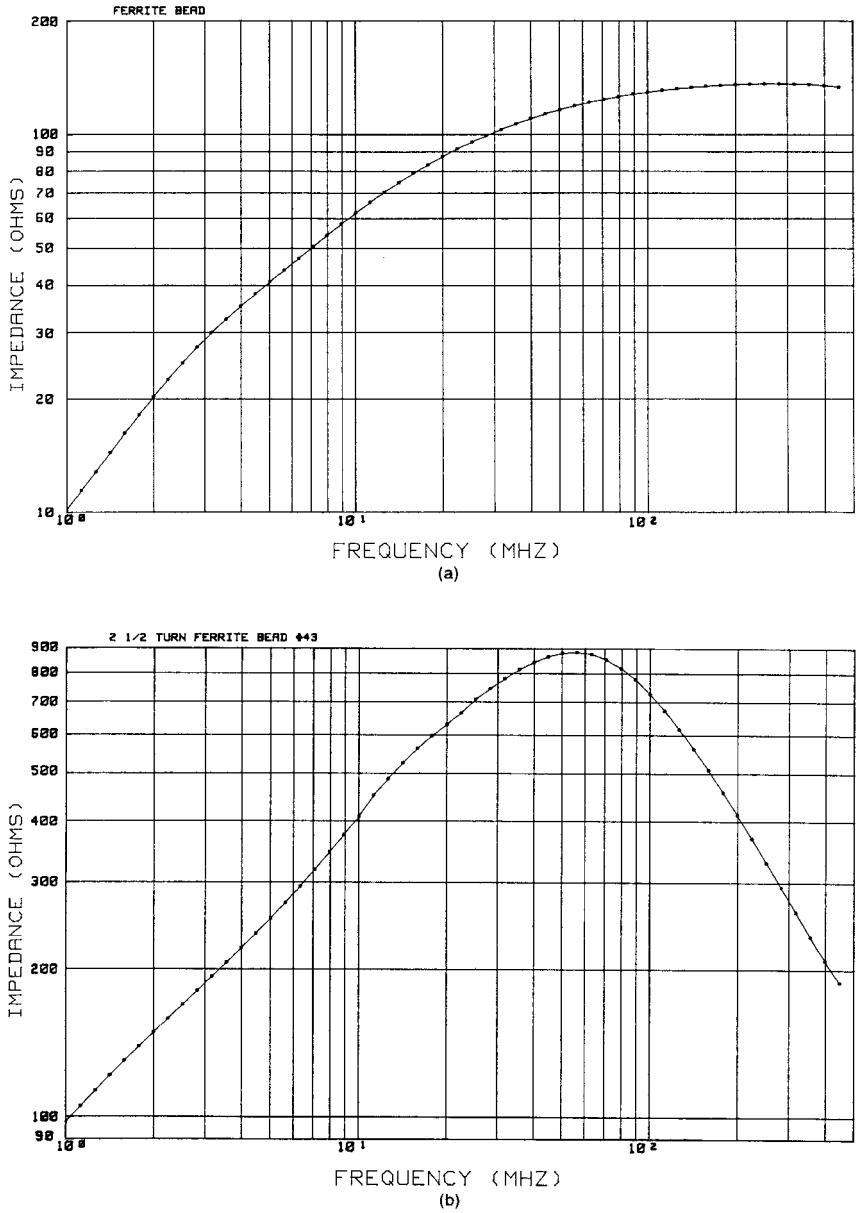

FIGURE 5.33 Measured impedances of (a) a $\frac{1}{2}$-turn ferrite bead and (b) a $2\frac{1}{2}$-turn ferrite bead.

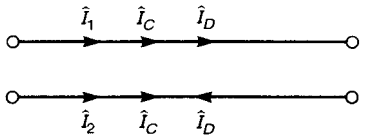

FIGURE 5.34 Decomposition of the currents on a two-wire transmission line into common-mode I_C and differential-mode I_D components.

as *differential-mode* $\hat{I}_D$ and *common-mode* $\hat{I}_C$:

$$\hat{I}_1 = \hat{I}_C + \hat{I}_D \tag{5.29a}$$

$$\hat{I}_2 = \hat{I}_C - \hat{I}_D \tag{5.29b}$$

Solving these two equations gives

$$\hat{I}_D = \tfrac{1}{2}(\hat{I}_1 - \hat{I}_2) \tag{5.30a}$$

$$\hat{I}_C = \tfrac{1}{2}(\hat{I}_1 + \hat{I}_2) \tag{5.30b}$$

The differential-mode currents $\hat{I}_D$ are equal in magnitude but oppositely directed in the two wires. These are the desired or functional currents. The common-mode currents $\hat{I}_C$ are equal in magnitude but are directed in the same direction. These are not intended to be present, but will be present in practical systems. Standard lumped-circuit theory does not predict these common-mode currents. They are frequently referred to as *antenna-mode currents*.

Let us now investigate the significance of each current on the radiated emissions from this pair of conductors, which may be wires or lands on a PCB. This will be investigated in more detail in Chapter 8. For the present it suffices to give a general discussion. The radiated electric fields $\hat{E}$ due to each current can be superimposed to give the total radiated electric field. First consider the radiated fields due to differential-mode currents, as illustrated in Fig. 5.35a. The differential-mode currents are oppositely directed. Thus the resulting electric field will also be oppositely directed. However, since the two conductors are not collocated, the fields will not exactly cancel, but will subtract to give a small net radiated electric field. On the other hand, since the common-mode currents are directed in the same direction, their radiated field will add, giving a much larger contribution to the total radiated field than will the differential-mode currents, as is illustrated in Fig. 5.35b. Thus *a small common-mode current can produce the same level of radiated electric field as a much larger value of differential-mode current.* In short, *common-mode currents have a much higher potential for producing radiated emissions than do differential-mode currents*! We will find in Chapter 8 that *the predominant mechanisms for*

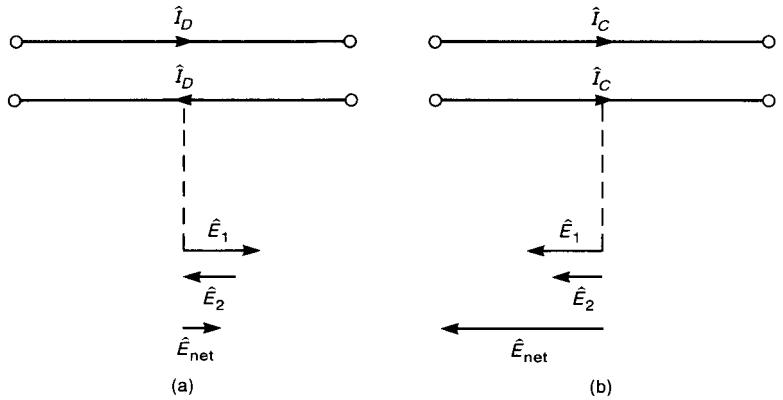

FIGURE 5.35 Illustration of the relative radiated emission potential of (a) differential-mode currents and (b) common-mode currents.

producing radiated electric fields in practical products are the common-mode currents on the conductors! For example, we will find that microamperes of common-mode current will produce the same level of radiated electric field as tens of milliamperes of differential-mode current! Common-mode currents are not intended to be present on the conductors of an electronic system, but nevertheless are present in all practical systems. Because of their considerable potential for producing radiated electric fields, we must determine a method for reducing them.

One of the most effective methods for reducing common-mode currents is with *common-mode chokes.* A pair of wires carrying currents $\hat{I}_1$ and $\hat{I}_2$ are wound around a ferromagnetic core as shown in Fig. 5.36a. Note the directions of the windings. The equivalent circuit is also shown. Here we assume that the windings are identical, such that $L_1 = L_2 = L$. In order to investigate the effect of the core on blocking the common-mode current, we calculate the impedance of one winding:

$$\hat{Z}_1 = \frac{\hat{V}_1}{\hat{I}_1} = \frac{pL\hat{I}_1 + pM\hat{I}_2}{\hat{I}_1} \tag{5.31}$$

Now let us investigate the contribution to the series impedance due to each component of the current. First let us consider common-mode currents in which $\hat{I}_1 = \hat{I}_C$ and $\hat{I}_2 = \hat{I}_C$. Substituting into (5.31) gives

$$\hat{Z}_{CM} = p(L + M) \tag{5.32}$$

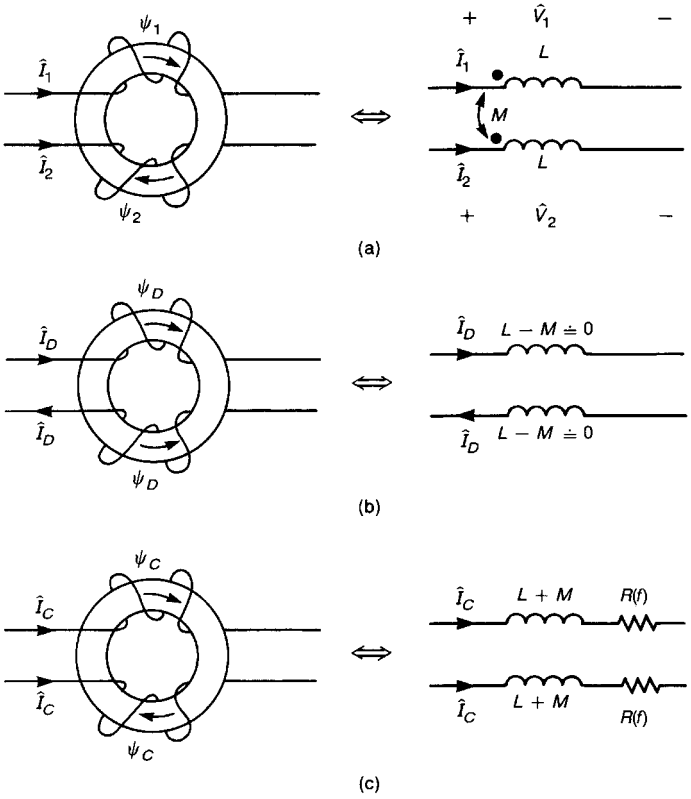

FIGURE 5.36 Modeling the effect of a common-mode choke on (a) the currents of a two-wire line, (b) the differential-mode components, and (c) the common-mode components.

The contribution to the series impedance due to differential-mode currents where $\hat{I}_1 = \hat{I}_D$ and $\hat{I}_2 = -\hat{I}_D$ is

$$\hat{Z}_{DM} = p(L - M) \tag{5.33}$$

If the windings are symmetric and all the flux remains in the core, i.e., the flux of one winding completely links the other winding, then $L = M$ and $\hat{Z}_{DM} = 0$! Thus in the ideal case where $L = M$ *a common-mode choke has no effect on differential-mode currents, but selectively places an inductance (impedance) 2L in series with the two conductors to common-mode currents.* These notions are illustrated in Fig. 5.36.

In addition to selectively placing inductors $L + M$ in series with the common-mode currents, use of ferrite cores places a frequency-dependent resistance, $R(f)$, in series with the common-mode currents as well. This resistance becomes dominant

at the higher frequencies as was the case for a ferrite bead in the previous section. Hence common-mode currents not only are blocked but also have their energy dissipated in the $R(f)$.

Thus common-mode chokes can be effective in blocking and dissipating common-mode currents. In order to provide this impedance to common-mode currents, the wires must be wound around the core such that the fluxes due to the two common-mode currents *add* in the core whereas the fluxes due to the two differential-mode currents *subtract* in the core. Whether the wires have been wound properly can be checked with the *right-hand rule*, where, if one places the thumb of one's right hand in the direction of the current, the fingers will point in the resulting direction of the flux produced by that current. A foolproof way of winding two wires (or any number of wires) on a core to produce this effect is to wind the entire group around the core as illustrated in Fig. 5.37a. In either case one should ensure that the wires entering the winding and those exiting the winding are separated from each other on the core, or else the parasitic capacitance between the input and output will shunt the core and reduce its effectiveness, as illustrated in Fig. 5.37b.

The effectiveness of the common-mode choke relied on the assumption that the self and mutual inductances are equal, $L = M$. High-permeability cores tend to concentrate the flux in the core and reduce any leakage flux. Symmetric windings also aid in producing this. Unfortunately, ferromagnetic materials suffer from *saturation* effects at high currents, as discussed earlier, and their permeabilities tend to deteriorate with increasing frequency more than low-permeability cores. One of the most important advantages of the common-mode choke is that *fluxes due to high differential-mode currents cancel in the core and do not saturate it.* The

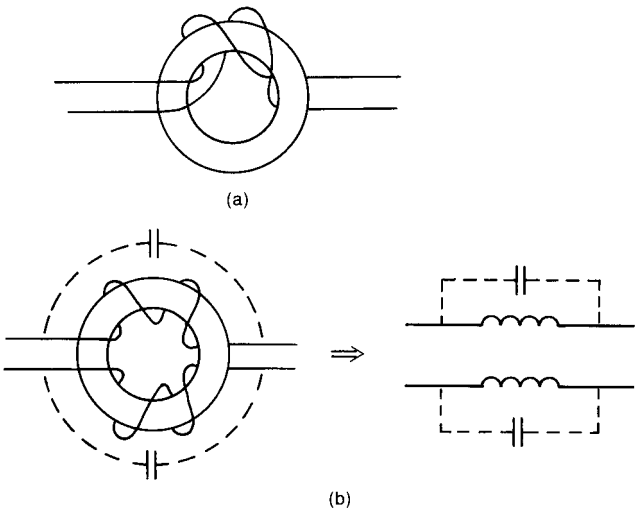

FIGURE 5.37 (a) A simple way of winding a common-mode choke; (b) parasitic capacitance.

functional or differential-mode currents $\hat{I}_D$ are the desired currents, and are usually large in magnitude. If the flux due to these high-level currents did not cancel in the core, the core would tend to saturate, and the high permeability would be lost. Thus more of the flux would leak out into the surrounding air, and the self and mutual inductances would not be approximately equal. Furthermore, since the differential-mode fluxes cancel in the core, the choke does not (ideally) affect the functional signal as do the other suppression components discussed previously. So *the functional signals are not (ideally) affected by the presence of the choke, and also do not affect the performance of the choke.*

5.10 ELECTROMECHANICAL DEVICES

A number of electronic products such as typewriters, printers, and robotic devices use small electromechanical devices such as dc motors, stepper motors, ac motors, and solenoids to translate electrical energy into mechanical motion. These seemingly innocuous (from an EMC standpoint) devices can create significant EMC problems. DC motors create high-frequency spectra due to arcing at the brushes as well as providing paths for common-mode currents through their frames. The purpose of this section is to highlight these problem areas and increase the awareness of the reader for their potential to create EMC problems.

5.10.1 DC Motors

DC motors are used to produce rotational motion, which can be used to produce translational motion using gears or belts. They rely on the property of magnetic north and south poles to attract and like poles to repel. A dc motor consists of stationary windings or coils on the *stator*, along with coils attached to the rotating member or *rotor*, as illustrated in Fig. 5.38a. The coils are wound on metallic protrusions, and a dc current is passed through the windings, creating magnetic poles. A commutator consists of metallic segments that are segmented such that the dc current to the rotor windings can be applied to the appropriate coils to cause the rotor to align with or repel the stator poles as the rotor rotates. Carbon brushes make contact with the rotor segments and provide a means of alternating the current and magnetic fields of the rotor poles using a dc current from a source, as illustrated in Fig. 5.38b. As the current to the rotor coils is connected and disconnected to the dc source through the commutator segments, arcing at the brushes is created as a result of the periodic interruption of the current in the rotor coils (inductors). This arcing has a very high-frequency spectral content, as we saw in Chapter 3. This spectral content tends to create radiated emission problems in the radiated emission regulatory limit frequency range between 200 MHz and 1 GHz, depending on the motor type. In order to suppress this arcing, resistors or capacitors may be placed across the commutator segments as illustrated in Fig. 5.38c. These can be implemented in the form of capacitor or resistor disks that are segmented disks of capacitors or resistors attached

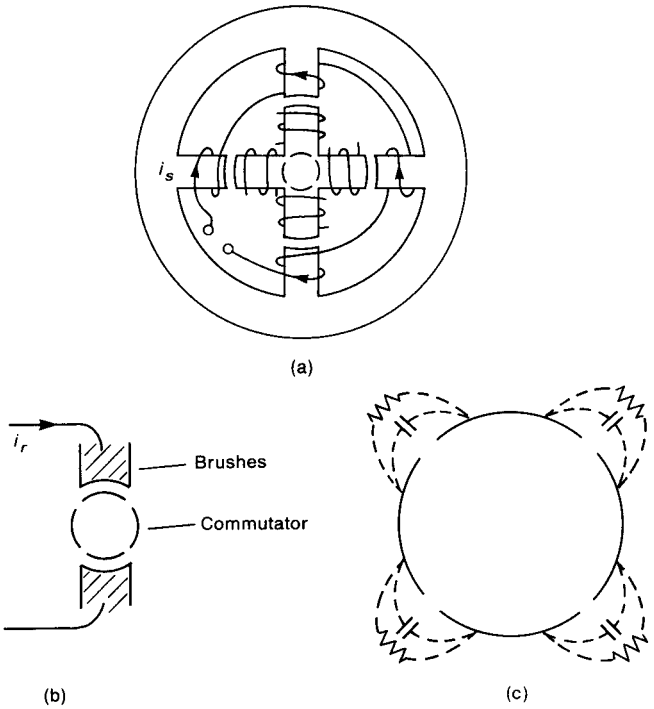

FIGURE 5.38 A dc motor illustrating (a) physical construction, (b) brushes and commutator, and (c) arc suppression elements.

directly to the commutator or in resistive ring placed around the commutator. In some cases it may be necessary to insert small inductors in the dc leads to block those noise currents that are not completely suppressed by the capacitor or resistor disks.

An additional source of high-frequency noise and associated radiated and conducted emission comes not from the motors themselves but from the *driver circuits* that are used to change the direction of rotation to provide precise position control of the motor. A typical "H-drive" circuit for a small dc motor is illustrated in Fig. 5.39a. When transistors T_1 and T_1' are turned on, current flows through the commutator and the rotor windings, causing the rotor to turn in one direction. When these are turned off and transistors T_2 and T_2' are turned on, the rotor turns in the opposite direction. This driver circuit is usually connected to the motor via a long pair of wires as shown in Fig. 5.39b. For reasons of thermal cooling of the motor, its housing is usually attached to the metallic frame of the product, which acts as a heat sink. This produces a large capacitance C_{par} between the motor housing and the product frame. This provides a path for *common-mode currents* to pass through the connection wires from the rotor to the stator via capacitance between these windings, and eventually to the frame via C_{par}. The current provided to the

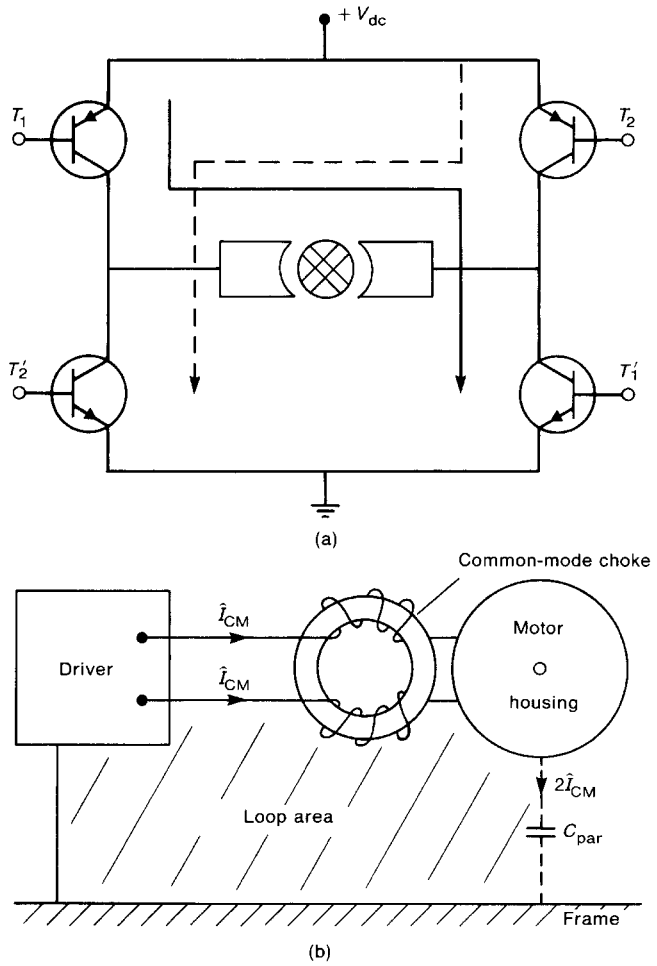

FIGURE 5.39 Illustration of (a) an H-drive circuit and (b) conversion of common-mode driver currents into differential-mode currents with a large loop area because of parasitic capacitance to the motor frame.

motor by the driver, although ideally intended to be dc, typically has fast-rise time spikes present on it due to the constant interruption of the current in the driver circuit and in the rotor coils by the commutator. These spikes have very high-frequency spectral content, which is then placed on the product frame and is coupled to other parts of the product radiating in the process. The loop area formed by the leads and their return path (the product frame) also tends to be quite large. We will find in Chapter 8 that the radiation potential tends to be a direct function of the loop area occupied by that current; the larger the loop area, the larger the radiated

emission. In order to block this common-mode current, a common-mode choke may be needed to be placed in the driver leads, as is illustrated in Fig. 5.39b. This shows a case where common-mode current (in the driver leads) becomes essentially a differential-mode current flowing around a large loop area. Measured common-mode impedances between the input wires (tied together) and the motor frame for a small dc motor give an impedance null around 100 MHz of about 1 Ω.

5.10.2 Stepper Motors

An alternative to the dc motor for electromechanical positioning is the *stepper motor.* There are basically two types of stepper motors: *permanent magnet* (PM) and *variable reluctance* (VR). Both types have dc current applied to the stationary windings of the stator to produce magnetic poles. The stator and the rotor are segmented into a large number of poles around their peripheries in order to provide fine positioning. The rotor of the PM stepper is permanent magnet made of rare-earth materials. The rotor of the VR stepper consists of shorted turns of wire. Flux from the stator induces currents in these shorted turns, which induces magnetic poles on the rotor. The windings of the stator are arranged in phases to provide various degrees of magnetic pole segmentation. The rotor poles tend to align with those of the stator that are energized in order to reduce the *reluctance* of the magnetic path.

Although there is no arcing to generate high-frequency signals as with the commutator of the dc motor, there remains the problem of common-mode currents between the driver circuit wires and the frame of the motor, which is again attached to the frame of the product for cooling. A typical driver circuit is shown in Fig. 5.40. Turning on transistors T_1 and T_4, for example, causes current to flow through the windings of phase A and phase D in the indicated direction, causing the motor to rotate to one desired position. Constant energization and deenergization of these stator windings again causes high-frequency noise to be passed down the connection wiring. As with other motors, parasitic capacitance exists between the input wires and the motor frame, which is attached to the product frame for thermal reasons. Thus the noise currents on the input wires are placed on the frame of the product and return to the driver via that path. This creates the same problem that was observed for dc motors, and may require that a common-mode choke be placed in the driver wires in order to block this path and reduce the radiated emissions of this common-mode current (which becomes a differential-mode current by passing through the large loop created by the driver wires–ground plane circuit). Measurements of the common-mode impedance between the input wires (tied together) and the motor frame for a typical small stepper motor show a null around 70 MHz of some 3 Ω!

5.10.3 AC Motors

AC motors are seldom used to provide positioning of mechanical elements as are dc and stepper motors, but rather are used to provide constant speed and drive small

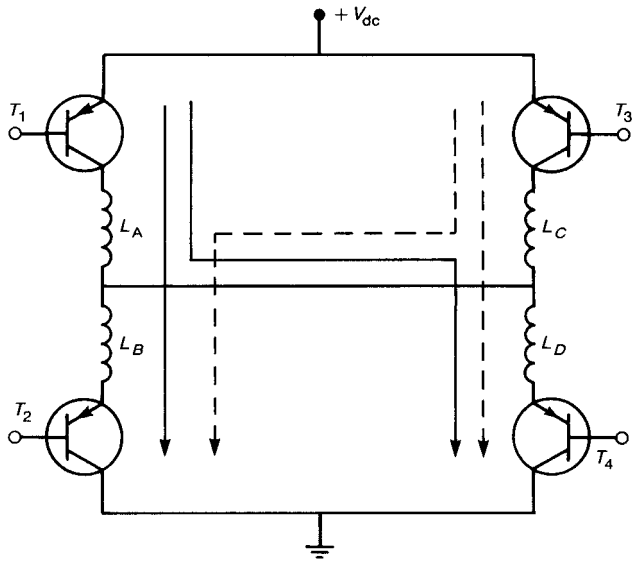

FIGURE 5.40 A typical driver circuit for a stepper motor.

cooling fans. The absence of brushes and the attendant arcing as with dc motors and the noise currents provided by the drivers of both dc and stepper motors tends to diminish the potential of these motors for creating noise problems as opposed to dc or stepper motors. However, because the rotor and stator of these motors consist of closely spaced inductors, there remains the problem of large parasitic capacitance between the rotor and the stator. If the motor frame is mechanically attached to other mechanical parts of the product, then the potential exists for coupling common-mode currents from the ac power source to the product frame and vice versa. If high-frequency noise is present on the ac waveform feeding these motors or the frame to which the stator is attached, then it is likely that this noise will be coupled to the product frame or to the ac power cord, where its potential for radiated or conducted emissions will usually be enhanced. Chopper drivers are frequently used to control the power to the ac motors. Thus the input current may have a high-frequency spectral content which is transferred via common mode to the product frame. Common-mode chokes in the attachment leads of these types of motors may be needed in order to block this path.

5.10.4 Solenoids

A *solenoid* is essentially a coil of wire with a ferromagnetic slug at its center. Energizing the coil with a dc current causes a magnetic flux to be generated. The ferromagnetic slug tends to move to the center of the coil in a translational fashion in order to minimize the reluctance of the magnetic path. These types of

electromechanical devices suffer from many of the problems of the abovementioned motors with the exception of commutation. Sudden energization and deenergization of the winding inductance creates high-frequency noise. Once again, the parasitic capacitance between the windings and the metallic housing of the solenoid creates a potential path for common-mode currents to be placed on the frame of the product, which may require a common-mode choke in the input leads. Measurement of the common-mode impedance between the input wires (tied together) and the solenoid frame for a small solenoid indicate a null at around 150 MHz of 8 Ω!

5.11 DIGITAL CIRCUIT DEVICES

Digital products are very popular today because of their ability to rapidly process data and their inherent noise immunity. However, these attributes pose problems for an EMC standpoint. Data are transmitted and processed in the form of pulses. The transitions between each state (the pulse rise/falltimes) tend to be extraordinarily fast (of order 1 ns). We saw in Chapter 3 that these fast transition times tend to generate high-frequency spectral content in the frequency-domain representation of these signals, which contributes to the high-frequency radiated and conducted emissions of the product. The requirement for increased speeds of data transmission and processing will no doubt cause these EMC concerns to increase in digital products in the future.

Digital products are relatively simple in architecture and typically consist of a central processor in the form of a microprocessor, which performs computation, stores and retrieves data and instructions, and provides sequencing of the entire processes. Various read-only-memory (ROM) modules provide nonvolatile storage of program instructions. Random-access-memory (RAM) modules provide for storage of data, and various drivers or buffers provide the ability to drive peripheral devices or communicate data. One or more *system clocks* provide synchronization of the occurrence of each task within well-defined windows of time. The primary task is to input data and instructions either from external devices such as tape or disk drives or from keyboards and to process this and provide the results as output to displays or signals to drive external processes such as motors or other actuators.

The process seems relatively straightforward from the standpoint of its effect on the EMC profile of the product. However, the subtle aspects of the process have considerable impact. For example, the particular technology and requirements of the product affect the rise/falltime of the clock and data pulses, which affect their high-frequency spectal content. Buffer gates are frequently provided to interface between low-current logic signals and high-current outputs. These have the effect of "squaring up" the signals. Suppose the rise/falltimes of a clock signal have been slowed by the insertion of a lowpass filter such as a shunt capacitor. If a buffer gate has been inserted at some point further down the line, the signal may be "squared up" and have current drive added, thus increasing its high-frequency spectral content.

Conductors that are intended to carry only "rare event" signals that only occur infrequently should not be overlooked since, *although they are not intended to carry high-frequency signals, they may have these present as a result of inadvertent coupling to these lines.* For example, the reset line of a microprocessor may be active only infrequently during machine operation. However, inadvertent coupling of other high-frequency signals to this line can cause very high-frequency signals to be present on this line. If the reset line is routed a long distance around the PCB, it may cause significant radiated emissions, which the EMC engineer may not suspect as being the source of the emissions. It is particularly instructive to probe points on a PCB of a digital product and observe the spectral content of the signals. Virtually all signal lines in a digital product should be suspect with regard to carrying high-frequency signals, although some (such as clock lands) are clearly of more importance. It is this author's experience that the most effective method of reducing radiated and conducted emissions is to affect the source of these emissions. Although this is a seemingly obvious point, it is nevertheless important to keep in mind. Once noise signals are allowed to propagate away from their source, their suppression becomes a problem of suppressing the emanation of the same signal from different points of emission resulting in the need for many more suppression elements.

The active digital components are composed of large number of semiconductor diodes, bipolar junction transistors (BJTs), and field-effect transistors (FETs). These are implemented in integrated circuit form on minute chips. One of the primary parasitic components of these elements that is of concern in EMC is the *parasitic capacitances* formed at the semiconductor junctions [9]. Each of these elements is formed from two types of semiconductor, *n*-type and *p*-type. This junction causes a separation of charge which acts like a capacitance. Once these parasitic capacitances are added to the ideal model of the device, it becomes clear that rise/falltimes of signals will be affected. Of more importance is the effect of these parasitic capacitances in *routing signals around the element*, in effect providing a direct connection at high frequencies from the input of the device to its output.

5.12 EFFECT OF COMPONENT VARIABILITY

It is very important to remember that it will always be required to produce a large number of supposedly identical copies of a product for sale. It is important and relatively simple to produce identical products from a functional standpoint; that is, all products are able to meet the functional performance design goals. This has always been and will continue to be an important criterion in the design process. However, consistency in achieving the EMC design goals among supposedly identical copies of a product is another matter that is not generally assured by achieving consistency in meeting the functional performance design goals. For example, suppose a product prototype is "fine-tuned" to meet the EMC regulatory limits on radiated and conducted emissions. Once the product is placed in production and a large number of copies are made, it is not assured that all of these "copies" will also meet EMC

regulatory limits, which require that *all units that are sold must comply*. Changes in parts vendors to reduce product cost can cause a product that previously was in compliance to suddenly be out of compliance, even though it continues to meet the functional performance objectives. One also must realize that the functional performance goals and the EMC performance goals are often in conflict. For example, functional designers are generally concerned about the *maximum rise/falltimes of a digital component*, whereas EMC designers are more concerned about the *minimum rise/falltimes of the digital component* since the shorter the rise/falltime, the larger the high-frequency spectral content of the signal. Manufacturers of components cannot guarantee absolute conformance to specifications of their components, but instead specify bounds. A digital component manufacturer may guarantee maximum rise/falltimes of his/her component for functional performance reasons. A large quantity of these parts used to produce "identical copies" of the product may (and usually do) exhibit variations that, although within the bounds specified by the part manufacturer, may exceed the bounds that are being relied on by the EMC engineer and cause one or more of the "copies" to be out of compliance.

Changing parts vendors to reduce cost at some point in the production cycle of the product can create compliance problems. An example is illustrated in [10]. An RS-232 line driver was tested for this type of variability. Several "equivalent" line drivers from different vendors were tested, and the spectrum present on the −12 V dc lead to each component was measured over the frequency range of 10–210 MHz. The reader is referred to that publication, which shows extreme variability in the emission present on the −12 V lead from vendor to vendor and within parts of the same vendor. All parts would no doubt meet the functional performance goals. Also observe that the −12 V lead of the line driver "is not supposed to carry these high-frequency signals," but does in fact have these present. This again illustrates that *just because a conductor is not intended to carry high- frequency signals does not rule out the presence of high-frequency signals on that conductor.*

5.13 MECHANICAL SWITCHES

Mechanical switches are often used in electronic products to provide the operator with a quick and easy way of changing the product behavior. On–off switches connect commercial power to the product. Other switches may simply provide a change in the status of the product, for example a reset switch on a personal computer. The EMC problems that may result from the activation of mechanical switches are quite varied, and depend strongly on the load that is switched. Arcing at the contacts is the primary interference problem since the arc waveform may contain very high-frequency spectral components of large magnitude, as we will see. Early investigations concerned the interruption of large currents by circuit breakers in power systems [11]. In the early 1940s work concentrated on the behavior of switches in telephone circuits with regard to erosion of the switch contacts as well as the interference produced by these operations [12–16]. In

order to subdue this potential interference problem and to insure longer life for the switch contacts, various protection networks are often used.

In this final section we will discuss the EMC aspects of mechanical switches. The discussion will be brief but will cover the essential points. For a more complete and thorough discussion of the subject the author recommends the text by Ott [6] as well as [11–16]. These references contain virtually all the information one needs to know about mechanical switches from the standpoint of EMC. The following is a condensed summary of that information.

5.13.1 Arcing at Switch Contacts

It has been known from before the days of the Marconi spark-gap transmitter that current in the form of an arc can be conducted between two electrodes that are immersed in air. For example, consider two contacts separated a distance d in air shown in Fig. 5.41. The typical voltage–current characteristic is shown. There are three regions shown: the Townsend discharge region named for its discoverer, the glow discharge region, and the arc discharge region. The various voltage levels are denoted as V_B, V_G, and V_A. Typical values for these variables for contacts in air are $V_B \cong 320\,\text{V}$, $V_G \cong 280\,\text{V}$, and $V_A \cong 12\,\text{V}$. The value of V_B depends on contact separation, while that of V_A depends on the contact material. The currents at the transition regions are denoted as I_G and I_A. These are quite variable, but are of order $I_G \cong 1$–100 mA and $I_A \cong 0.1$–1 A.

There are always a few free electrons in the space between the contacts due to cosmic radiation, photon collisions with the gas molecules, etc. As the voltage between the two contacts is increased, the resulting electric field between the contacts accelerates these free electrons, causing them to strike neutral gas molecules. If the free electrons have sufficient kinetic energy imparted by the electric field, they strike the gas molecules, creating additional free electrons as electron–ion pairs. The field accelerates these newly formed electrons, causing them to strike other gas molecules and thereby releasing more free electrons. This produces a multiplicative production of free electrons and positive ions. The positive ions move toward the cathode (the negative terminal of the contact) and the electrons move toward the anode (the positive terminal of the contact). As the positive ions move toward the cathode, they create a space charge around it that increases the local field and the production of free electrons. The positive ions also strike the cathode, liberating more free electrons by secondary emission. This mechanism characterizes the Townsend discharge region of Fig. 5.41. Thermionic heating of the cathode can also liberate electrons, but this mechanism tends to predominate at the higher currents of the arc discharge region. In the early, low-current region all of the electrons emitted at the cathode are collected by the anode. Above a certain voltage level all electrons emitted by the cathode are collected, independently of further increases in voltage, and the curve rises vertically. At still higher voltages the electrons acquire sufficient kinetic energy to create electron–ion pairs in their collisions with the gas molecules, thereby increasing the free electrons and

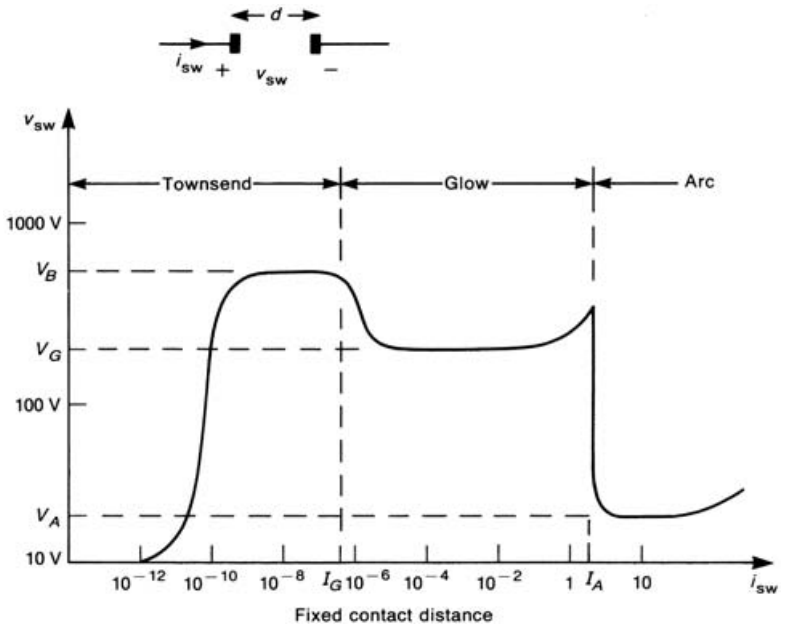

FIGURE 5.41 Illustration of the voltage–current characteristic of arcing at mechanical contacts.

resulting in an avalanche effect. The peak or *breakdown* voltage V_B is dependent on the gas, contact separation and pressure. Paschen found that the breakdown voltage was dependent on the product of the pressure and the contact separation distance as [11]

$$V_B = \frac{K_1 pd}{K_2 + \ln pd} \tag{5.34}$$

where K_1 and K_2 are constants that depend on the gas. For air at standard atmospheric pressure the minimum breakdown voltage is approximately $V_{B,\min} \cong 320\,\text{V}$ and occurs at a contact separation $d_{\min} = 0.3$ mils $= 0.00762$ mm.

At the peak of the Townsend discharge region the production of free electrons and positive ions reaches a self-sustaining, *avalanche* stage wherein the current is sustained by this avalanching process but the voltage across the contacts drops to the lower *glow voltage* designated as V_G. For contacts in air at atmospheric pressure $V_G \cong 280\,\text{V}$. A region near the cathode develops a faint glow, which is the origin of the term. The voltage drop across the switch remains constant at V_G for a large range of current and is primarily determined by the region between the cathode and the beginning of the glow region: the *cathode fall region.* As the current increases,

the dimension of the glow region increases toward the anode, but the voltage drop across the gap remains at V_G.

When the current increases sufficiently such that the cathode fall region encompasses the entire cathode area, further current increases result in higher current density. This leads to heating of the cathode and a slight increase in gap voltage. A point is reached rather quickly where the heating causes vaporization of the contact metal, resulting in a rapid drop in contact voltage, which marks the beginning of the *arc discharge region* where an arc forms between the contacts. The contact voltage drops to a very low voltage of about $V_A \cong 12\,\text{V}$. The value of V_A is determined by the contact material (since vaporization of the metal is the important process here) but is of about 11–16 V. Once the arc is initiated, a very luminous discharge results where further increases in current do not result in any appreciable change in the contact voltage from V_A. This is the usual visual effect one sees which contacts are opened and an arc forms momentarily.

The formation of an arc as discussed above was initiated by voltages large enough to cause breakdown of the intervening gas. The voltage across the contacts divided by the contact spacing exceeds the breakdown field strength of the gas. This is referred to as a *long arc*. For smaller contact spacings in a vacuum the arc can be initiated by a *field-induced emission* wherein the electric fields at the highest and sharpest points on the cathode liberate electrons. This electron stream fans out as it crosses the gap. Bombardment of the anode by this electron stream causes it to heat to several thousand kelvin, which is sufficient to vaporize the electrode. The cathode may vaporize first, depending on the contact sizes, rate of heating, etc. As the positive ions move toward the cathode, a space charge forms that further promotes the emission, resulting in an avalanche effect. Thus an arc may be formed where the voltage and contact spacing are not sufficient for a gas breakdown. This is referred to as a *short arc* or *metal–vapor arc discharge*. The required field strength is of order $E_B = 10^9$ V/m, although this varies, depending on the cleanliness of the contact surface and surface contaminants.

Figure 5.42 summarizes the breakdown voltage of a switch with air as the intervening medium. The plot is shown as a function of the contact separation distance d. Dividing the separation distance by the velocity of contact closure or opening v gives the axis as a function of time t. For small contact separations less than d_c a short arc may form if the contact voltage divided by the contact separation equals $E_B \cong 10^9\,V/m$. The contact voltage drops to $V_A \cong 12\,\text{V}$. The current through the switch is determined solely by the circuit voltage and impedance. However, a minimum current I_A is required to sustain the arc. This *minimum arc current* is quite variable, and ranges from tens of milliamperes to 1 A. *If the voltage across the contact available from the external circuit drops below V_A and/or the current through the contact available form the external circuit drops below I_A, the arc is extinguished.* For contact separations larger than d_c a glow discharge will form if the contact voltage exceeds the breakdown voltage, which is given by [12]

$$V_{B,\,\text{glow}} = 320 + 7 \times 10^6 d \tag{5.35}$$

This is essentially the Paschen voltage curve for $d > d_{\min}$. If the current available from the external circuit exceeds the *minimum glow discharge sustaining current* I_G, a glow discharge will form, and the contact voltage will drop to [12]

$$V_G = 280 + 1000d \tag{5.36}$$

If the current available from the circuit exceeds the minimum arc-sustaining current I_A, the glow discharge will transition to a *long arc*, and the contact voltage will again drop to $V_A \cong 12\,\text{V}$. It must be reemphasized that, *in order to sustain a glow* (*arc*) *discharge, the voltage across and current through the contact that are available from the external circuit must exceed* V_G *and* I_G (V_A *and* I_A). Again, the minimum sustaining voltages are rather predictable as $V_G \cong 280\,\text{V}$ and $V_A \cong 12\,\text{V}$, whereas the minimum sustaining currents I_G and I_A are quite variable. Some representative ranges are $I_G \cong 1$–100 mA and $I_A \cong 100$ mA–1 A. *The glow discharge is characterized by large voltage and small current, whereas the arc discharge* (*long or short arc*) *is characterized by low voltage and large current*.

It is interesting to observe that, although the physics of the two processes are quite different, the arc discharge of a mechanical switch has characteristics very similar to the silicon-controlled rectifier (SCR). Consider the voltage–current characteristic of the switch shown in Fig. 5.41. If we plot this only for large currents above a few milliamperes, the characteristic resembles that of a SCR. In fact, the operation of the two are quite similar. In order to "fire" an SCR, the voltage must be increased to the breakover point. Once the SCR fires, its voltage drops to a low value and the current increases substantially. The SCR can be turned off only by reducing its current below the "hold on current." The arc discharge of a mechanical switch is similar. In order to create an arc, the voltage across the switch must exceed the breakdown curve shown in Fig. 5.42. Once the arc forms, reducing the switch voltage cannot extinguish the arc (unless it is reduced below the arc voltage V_A). If the current is reduced below the minimum arcing current I_A, the arc will be extinguished!

5.13.2 The Showering Arc

Switches are frequently used to interrupt inductive loads such as solenoids or motors. Interruption of these types of loads leads to an interesting phenomenon known as the "showering arc", illustrated in Fig. 5.43. The inevitable parasitic capacitance is shown in parallel with the inductive load. When the switch is closed, a steady-state current $I_L = V_{\text{dc}}/R_L$ is established in the inductor. When the switch opens, the inductor attempts to maintain this current. It is therefore diverted through the capacitance, charging the latter. The switch voltage $v_{\text{sw}}(t) = v_C(t) + V_{\text{dc}}$, and therefore increases. As this switch voltage increases, it may exceed the switch breakdown voltage, whereby a short arc forms and the switch voltage drops to V_A. The capacitor discharges through the switch, with the current being primarily limited by the local resistance and inductance of the switch wiring. If the switch current exceeds the minimum arc-sustaining current, the arc is sustained. If not,

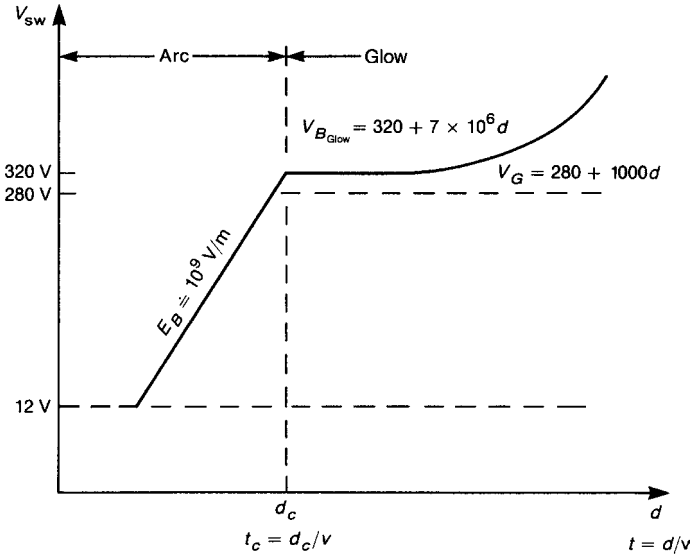

FIGURE 5.42 The breakdown voltage versus contact separation for a mechanical switch.

the arc is extinguished, and the capacitor begins to recharge. The switch voltage once again exceeds the switch breakdown voltage, and the switch voltage drops to V_A. If the arc is not sustainable, the capacitor begins to recharge once again. Eventually the energy stored initially is dissipated, and the capacitor voltage decays to zero, leaving $v_{sw} = V_{dc}$. This leads to a sequence of rising (as the capacitor charges) and rapidly falling (as the switch breaks down) voltages across the contacts, which has been referred to as the *showering arc* [15,16]. As the contact separation increases, a glow discharge may develop and may or may not be sustainable, resulting in miniature showering arcs, as illustrated in Fig. 5.43. The number and duration of each showering arc depends on the circuit element values and any delays associated by interconnection transmission lines. A SPICE model useful for predicting the arcing at switches and associated crosstalk is described in [17].

5.13.3 Arc Suppression

Showering arcs clearly have significant spectral content, and may therefore create EMC problems. The wiring carrying these currents may cause significant radiated emissions, thereby creating interference problems. These signals may also be directly conducted along interconnected wiring paths, creating a potentially more troublesome effect, since the signal levels that are directly conducted to other points will be of the order of the switch voltages, which may be several hundred

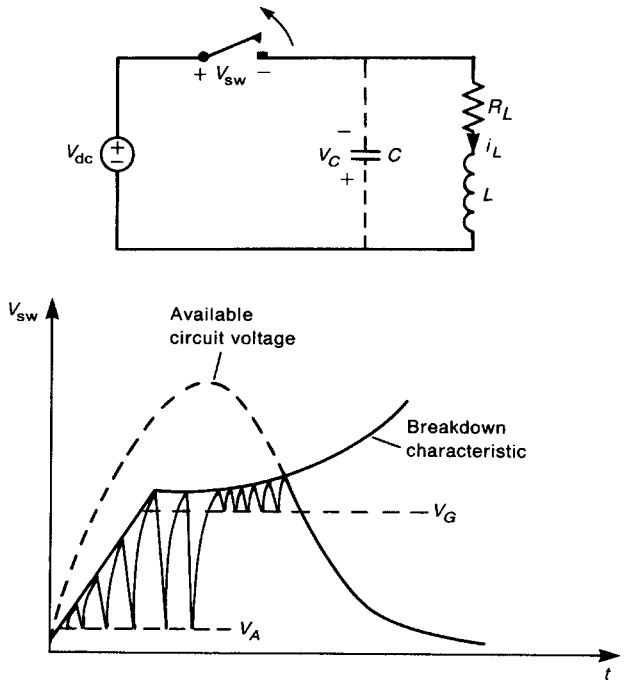

FIGURE 5.43 The showering arc for an inductive load.

volts. Since these potential effects are recognized, various suppression measures are usually employed in conjunction with a mechanical switch.

There are so many unknowns involved that it is difficult to make precise calculations. For example, velocity of switch closure or opening has a significant effect on the levels and duration of the showering arc. When the capacitor in Fig. 5.43 discharges through the switch, the discharge current is limited only by the impedance of the local wiring, which is quite small and substantially unknown and variable. Thus contact protection is usually based on simple calculations that reveal starting values to be used and then using an experimental test. In either event, the goal of contact protection is to *prevent the formation of an arc* (*sustained or showering*). Generally, either of two methods may be employed [6]: (1) prevent the switch voltage from exceeding the glow breakdown voltage of the switch (which is approximately 320 V), or (2) ensure that the arc current is below the minimum arc-sustaining current. Technique 1 prevents the arc from forming, while 2 prevents it from being sustained. There are two methods for implementing 1, as illustrated in Fig. 5.44. The contact breakdown voltage profile is plotted against the available circuit voltage (in the absence of breakdown). The slope of the arc breakdown characteristic, $d < d_c$, is obtained as the product of $E_B v$. Choosing $E_B = 10^8$ V/m

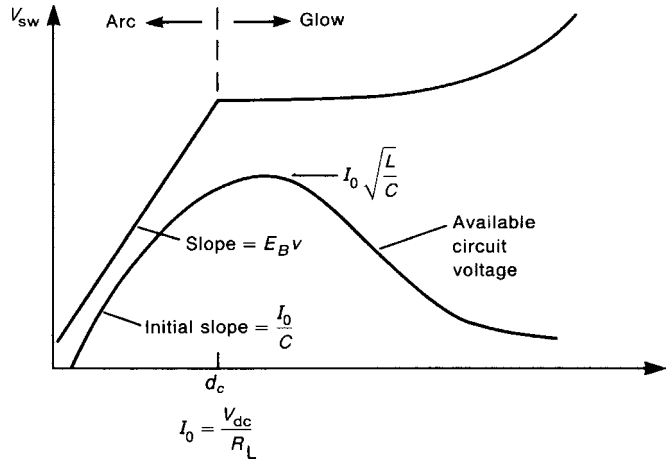

FIGURE 5.44 Contact protection by reducing the circuit available voltage.

and a typical switch velocity $v = 0.01$ m/s gives a slope of 1 V/μs. The initial slope of the available circuit voltage for the circuit of Fig. 5.43 can be shown to be I_0/C, where $I_0 = V_{dc}/R_L$ is the initial current through the inductor. Thus the initial rise of contact voltage should be kept below 1 V/μs, although this number is quite variable, depending on the contact surface (which affects E_B) and the contact approach velocity. The peak value of the available circuit voltage can be shown to be $I_0\sqrt{L/C}$ by neglecting the resistance R_L and assuming that all the energy stored in the inductor, $\frac{1}{2}LI_0^2$, is transferred to the capacitor, $\frac{1}{2}CV_{peak}^2$. In addition, the discharge waveform will be nonoscillatory (overdamped) if $\sqrt{L/C} < \frac{1}{2}R_L$ [5]. Even though an arc discharge can be avoided by slowing the initial rise of the available circuit voltage, a glow discharge (which may transition to a long arc discharge) may develop if the peak available circuit voltage exceeds the gas discharge breakdown threshold. Therefore, in order to prevent initiation of an arc, the following two criteria should be satisfied:

$$\text{(a)} \quad E_B v > \frac{V_{dc}}{R_L C}$$

$$\text{(b)} \quad \frac{V_{dc}}{R_L}\sqrt{\frac{L}{C}} < V_{B,\,gas} \cong 320 \text{ V}$$

This can be implemented by placing a sufficiently large capacitor in parallel with the inductor or the switch to increase the net capacitance, thereby reducing the peak available circuit voltage and also reducing the initial rise of the available circuit voltage as shown in Fig. 5.45a. This scheme has a significant drawback in that contact damage during switch closure may be significant because of the large

capacitor charging current. When the switch is open, the capacitor charges to the supply voltage V_{dc}. When the switch closes, this initial voltage discharges through the switch, which results in a large current surge through the switch.

Figure 5.45b shows how to remedy this problem caused by a single capacitor across the switch contact—place a resistor in series with the capacitor to limit the discharge current that occurs on contact closure. Limiting this discharge current on switch closure to below I_A gives the minimum value of the resistance. On contact opening, it is desirable to have the resistance as small as possible so as to not limit the arc suppression of the capacitor. The minimum value of R is chosen to limit the discharge current during switch closure to below the minimum arcing current: $V_{dc}/R < I_{A,min}$. The maximum value is determined by the opening of the switch. When the switch opens, the current is diverted through the resistor, and the switch voltage is I_0R, where $I_0 = V_{dc}/R_L$ is the initial current through the inductor. Usually the maximum value of R is chosen to be equal to R_L in order to limit the contact voltage to at most the supply voltage. Therefore the limits on choice of R are [6]

$$\frac{V_{dc}}{I_{A,min}} < R < R_L \tag{5.37}$$

The capacitor is chosen to satisfy the two criteria mentioned above: (1) the initial rate of voltage rise of the available circuit voltage, I_0/C, is less than 1 V/μs to avoid an arc forming; and (2) the peak available voltage, $I_0\sqrt{L/C}$, is less than 320 V to avoid a gas breakdown, which may transition to an arc. This leads to values C that must satisfy [6]

$$(1) \quad C \geq \left(\tfrac{1}{320} I_0\right)^2 L \tag{5.38a}$$

$$(2) \quad C \geq I_0 \times 10^{-6} \tag{5.38b}$$

A better but slightly more expensive network is shown in Fig. 5.45c [6]. A diode is placed across the resistor. While the switch is open, the capacitor charges up with polarity shown. When the switch closes, the resistor R limits the discharge current. When the switch opens, the diode shorts out the resistor, and the capacitor momentarily diverts the load current as described above. The capacitor value is chosen as above, but the resistor value is chosen to limit the current on closure to be less than the minimum arcing current:

$$R \geq V_{dc}/I_{A,min}$$

Contact suppression can be employed across the switch as described previously or across the inductive load, or both: An example of applying a diode across an inductive load is shown in Fig. 5.46a. When the switch opens, the inductor current is diverted through the diode rather than the switch. Contact arcing during switch closure is not affected. A common example of protection of inductive loads with a diode is in switching transistors. A diode ("freewheeling" diode) is placed across the inductive load, which may represent the inductance of a dc motor as shown in Fig. 5.46b. When the transistor switch interrupts the current through the inductance I_L, the inductance kick or Faraday's law voltage across the inductor causes the diode to short out.

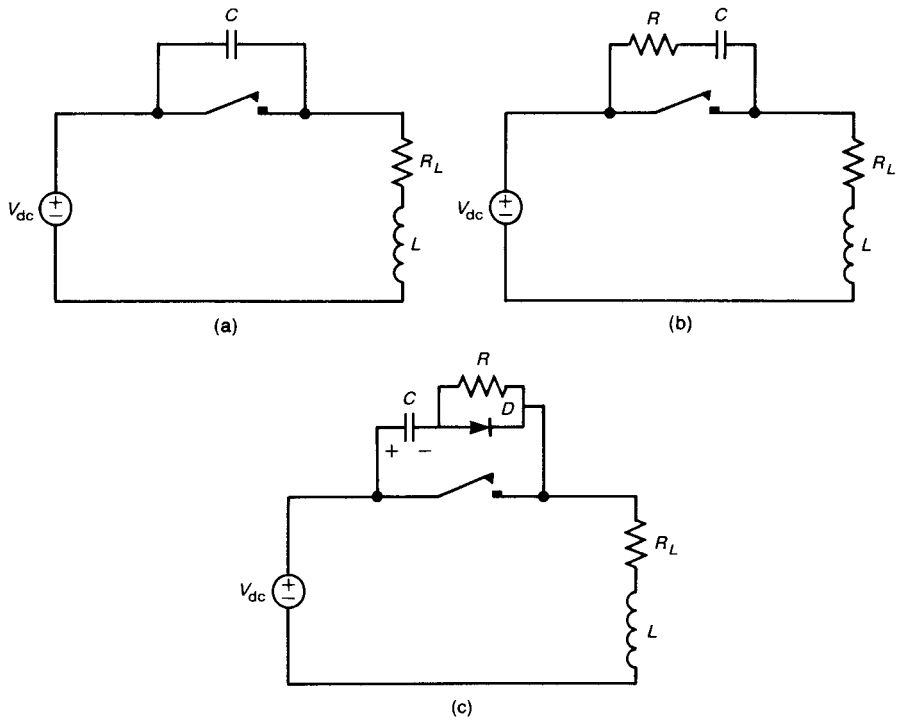

FIGURE 5.45 Various contact protection schemes: (a) capacitor; (b) $R-C$, (c) $R-C$ with a diode.

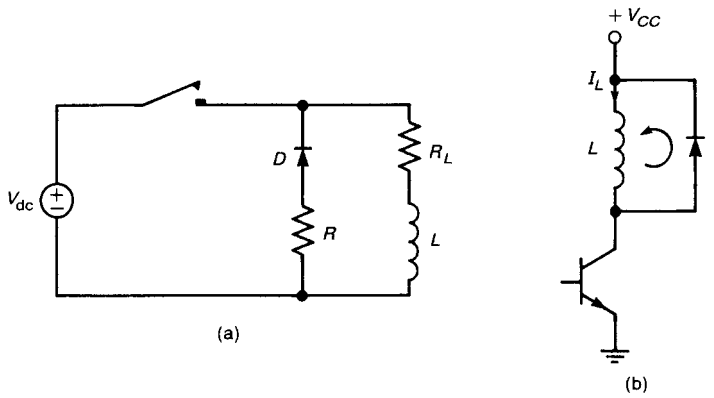

FIGURE 5.46 Diode protection for an inductive load.

Thus the diode clamps the collector of the transistor to $+V_{CC}$, preventing large collector–emitter voltages, which may destroy the transistor. Currents of larger magnitude and fast rise times will circulate around the inductor–diode loop. Therefore the diode must be placed very close to the inductor in order to minimize the loop radiation of this current loop.

Contact protection may or may not be required for resistive loads. If the load draws less than the minimum arcing current, no arc can be sustained, and no contact protection is generally required. If the resistive load draws a current greater than the minimum arcing current, a contact protection circuit similar to that of Fig. 5.45 may be required.

PROBLEMS

Section 5.1 Wires

5.1.1 Calculate the per-unit-length dc resistance of the following wires: #6 AWG (solid and 259 × 30), #20 AWG (solid and 19 × 32), #28 AWG (solid and 7 × 36), #30 AWG (solid and 7 × 38). [1.3 mΩ/m, 1.31 mΩ/m, 33.2 mΩ/m, 28 mΩ/m, 214.3 mΩ/m, 194.4 mΩ/m, 340.3 mΩ/m, 303.8 m Ω/m]

5.1.2 Determine the skin depth of steel (SAE 1045) at 1 MHz, 100 MHz, and 1 GHz. [0.26 mils, 0.026 mils, 0.00823 mils]

5.1.3 Determine the frequency where the resistance of a #20 AWG solid wire begins to increase because of the skin effect. [105.8 kHz] Determine the resistance of this wire at 100 MHz. [1.022 Ω/m]

5.1.4 Determine the frequency where the internal inductance of a #32 AWG solid wire begins to decrease due to skin effect. [1.7 MHz] Determine the internal inductance of this wire at 100 MHz. [6.5 nH/m or 0.165 nH/in.]

5.1.5 Determine the resistance, internal inductance, external inductance and capacitance of a typical ribbon cable consisting of two #28 AWG (7 × 36) wires 2 m in length and separated by 50 mils at 100 MHz. [3.74 Ω, 5.95 nH, 1.518 μH, 29.28 pF] Determine the characteristic impedance of the cable. [227.7 Ω]

5.1.6 Determine the resistance of a 6-in. PCB land of width 5 mils at 1 MHz and at 40 MHz. [0.59 Ω, 0.776 Ω]

Section 5.2 Printed Circuit Board (PCB) Lands

5.2.1 Determine the effective dielectric constant and characteristic impedance of a microstrip line constructed of a glass epoxy board of thickness of 47 mils supporting a 1-oz (ounce) Cu land 100 mils in width. [3.625, 45.3 Ω] Determine the per-unit-length inductance and capacitance. [7.3 nH/in., 3.56 pF/in.]

5.2.2 Determine the effective dielectric constant and characteristic impedance of a coplanar stripline constructed of a glass epoxy board of thickness 47 mils supporting two 1-oz Cu lands 100 mils in width and separated (edge to edge) by 100 mils. [1.96, 172.2 Ω] Determine the per-unit-length inductance and capacitance. [20.4 nH/in., 0.688 pF/in.]

5.2.3 Determine the characteristic impedance of two 1-oz Cu lands 100 mils in width that are located on opposite sides of a 47-mil glass epoxy board. [56.48 Ω]

Section 5.4 Resistors

5.4.1 The magnitude of an impedance is sketched as a Bode plot in Fig. P5.4.1. Determine one possible impedance expression for this. [$\hat{Z}(p) = 0.8(p + 3)/(p^2 + 10p)$]

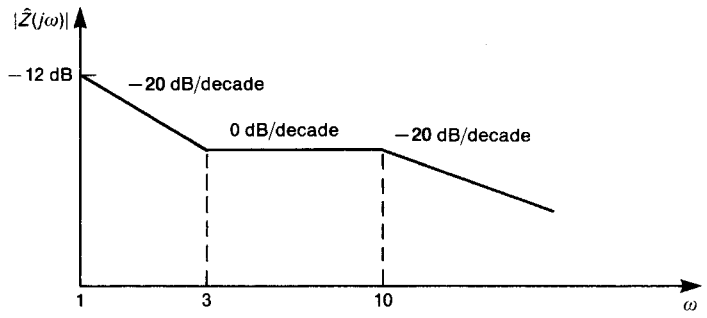

FIGURE P5.4.1

5.4.2 The magnitude of an impedance is sketched as a Bode plot in Fig. P5.4.2. Determine one possible impedance expression for this. [$\hat{Z}(p) = 18p(p + 30)/(p + 10)^2$]

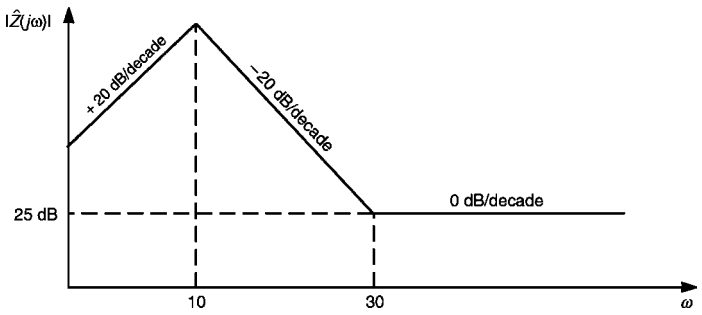

FIGURE P5.4.2

5.4.3 A $\frac{1}{8}$-W carbon resistor has the measured Bode plot of the impedance shown in Fig. P5.4.3. Determine the lead inductance and parasitic capacitance. [$L_{\text{lead}} = 12.48$ nH, $C_{\text{par}} = 5.64$ pF]

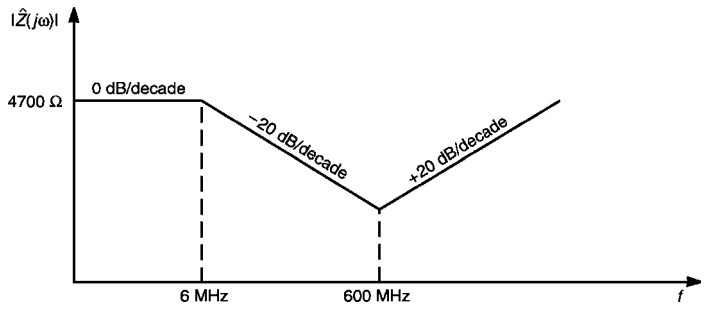

FIGURE P5.4.3

5.4.4 Calculate the parasitic capacitance for the 1000-Ω resistor directly from the measured data in Fig. 5.12a. [$C_{\text{par}} = 1.447$ pF]

5.4.5 A component is measured and found to have the impedance whose magnitude is shown in Fig. P5.4.5. Synthesize an equivalent circuit to represent this impedance. [100-Ω resistor in parallel with 15.92-μH inductor] Verify this using PSPICE.

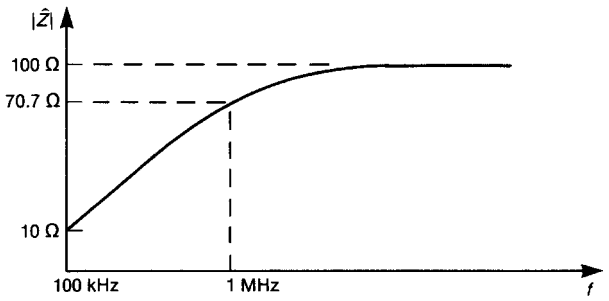

FIGURE P5.4.5

5.4.6 A component is measured and found to have an impedance whose (asymptotic) frequency response is shown in Fig. P5.4.6. Synthesize an equivalent circuit to represent this impedance. [1-nH inductor in series with the parallel combination of a 100-Ω resistor and a 1-μF capacitor] Verify this using PSPICE.

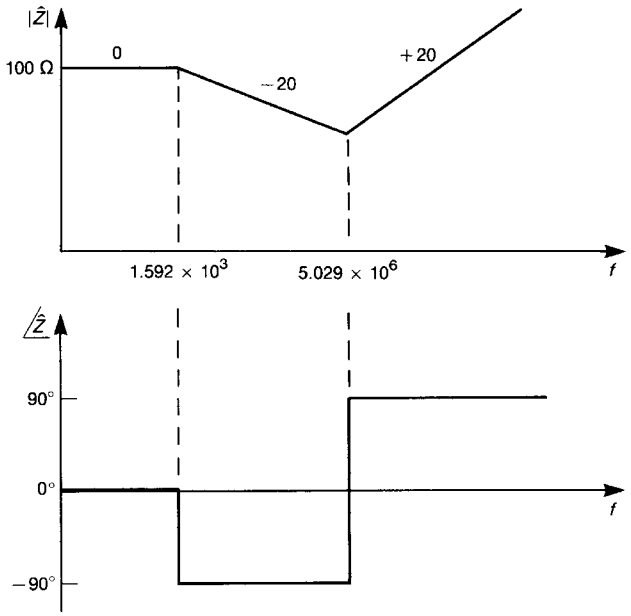

FIGURE P5.4.6

5.4.7 A component has the measured input impedance shown in asymptotic form in Fig. P5.4.7. Synthesize an equivalent circuit to represent this component at its terminals. [A 100-Ω resistor in series with a 0.01-μF capacitor] Verify this using PSPICE.

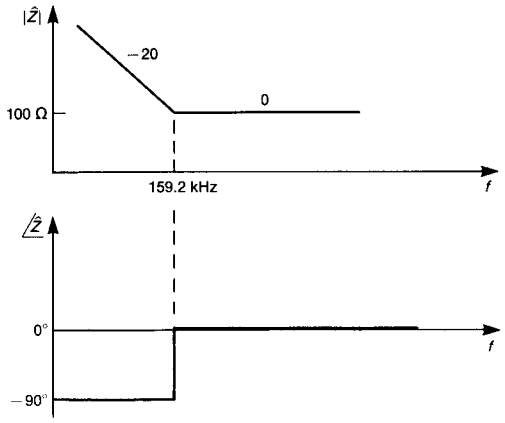

FIGURE P5.4.7

Section 5.5 Capacitors

5.5.1 Determine the lead inductance of the capacitor with very short leads whose measured data are as shown in Fig. 5.18. [4.775 nH]

5.5.2 A 100-MHz noise signal is being applied to the input of a transistor amplifier whose input impedance is $60\underline{/0^\circ}\ \Omega$ at 100 MHz. Determine the value of a capacitor that, when placed across the input, will divert 60% of this current. [20 pF] Confirm this using PSPICE.

5.5.3 A 50-Ω, 100-MHz sinusoidal source is terminated in a 50-Ω load resistor. Determine the value of a capacitor that when placed across the output will reduce the voltage by 20 dB. [633.4 pF]. Confirm this using PSPICE.

Section 5.6 Inductors

5.6.1 Determine the parasitic capacitance for the 1.2-μH inductor directly from the measured data in Fig. 5.25. [1.6 pF]

5.6.2 An inductor is to be placed in series with a 50-Ω load to block a 100 MHz noise current. Determine a value for the inductance that will reduce the 100-MHz noise signal across the load by 20 dB. [0.8 μH] Confirm this using PSPICE.

Section 5.7 Ferromagnetic Materials—Saturation and Frequency Response

5.7.1 For the toroid of NiZn whose measured impedance is shown in Fig. 5.30b, model the impedance as an inductor in parallel with a resistance that is in parallel with a parasitic capacitance of the windings. Determine the inductance, resistance, and parasitic capacitance directly from these measured data. [$L = 8\ \mu\text{H}$, $R = 1200\ \Omega$, $C_{\text{par}} = 1.6$ pF] Confirm this using PSPICE.

5.7.2 For the NiZn toroid whose measured impedance is shown in Fig. 5.30b, estimate the relative permeability of the material if there are 4 turns of wire, the core cross section is 0.5×0.5 cm, and the mean radius of the core is 1 cm. [$\mu_r \cong 1000$]

Section 5.8 Ferrite Beads

5.8.1 For the $\frac{1}{2}$-turn ferrite bead whose measured impedance is shown in Fig. 5.33a, determine the equivalent inductance. [$L = 1.6\ \mu\text{H}$]

5.8.2 For the $2\frac{1}{2}$-turn ferrite bead whose measured impedance is shown in Fig. 5.33b, determine the stray capacitance. [$C = 1.989$ pF]

Section 5.9 Common-Mode Chokes

5.9.1 An ideal common-mode choke (windings perfectly symmetric and having no losses) is constructed as shown in Fig. P5.9.1. With terminals AB connected, the impedance seen looking into terminals ab is $300{,}000\angle 90^\circ\ \Omega$ at 50 MHz. With terminals Ab connected, the impedance at 50 MHz seen looking into terminals aB is $10^6\angle 90^\circ\ \Omega$. Determine the self and mutual inductances of the choke. [$L = 1.035$ mH, $M = 0.557$ mH] Verify your result using PSPICE.

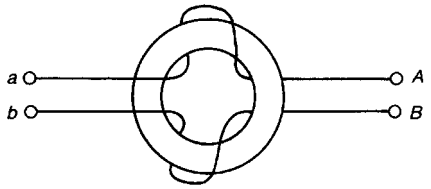

FIGURE P5.9.1

5.9.2 An ideal common-mode choke (windings perfectly symmetric and having no losses) is connected between a source and load as shown in Fig. P5.9.2. Determine the amplitude of the load voltage, assuming that all common-mode currents have been eliminated by the common-mode choke. [$2.564\angle -75.14^\circ$ V] Verify your result using PSPICE.

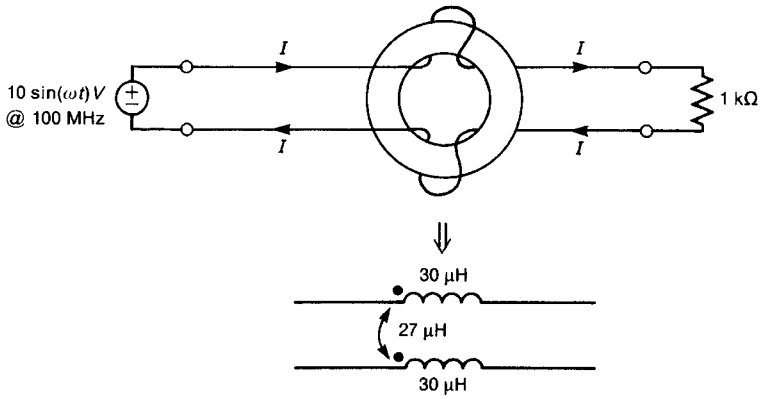

FIGURE P5.9.2

Section 5.10 Electromechanical Devices

5.10.1 A small dc motor has the input impedance frequency response shown in asymptotic form in Fig. P5.10.1. Synthesize an equivalent circuit to

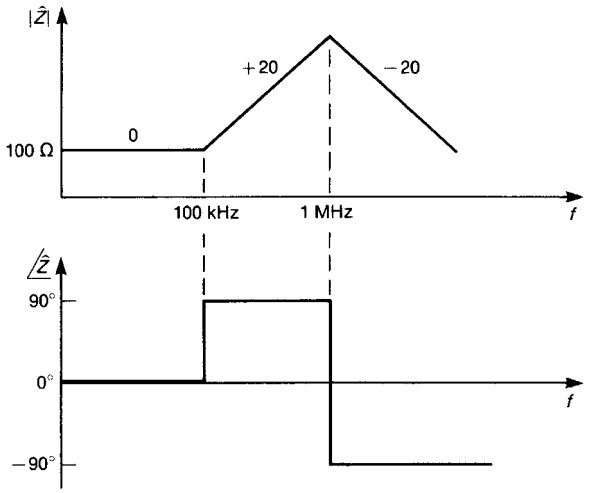

FIGURE P5.10.1

represent this motor at its input terminals. [159 pF in parallel with the series combination of 100 Ω and 159 μH] Verify your result using PSPICE.

Section 5.13 Mechanical Switches

5.13.1 For the $R-C$ switch protection network of Fig. 5.45b, suppose that $V_{dc} = 50$ V, $R_L = 500\,\Omega$, $L = 10$ mH, $I_A = 0.25$ A, and the switch closure/opening velocity is 0.01 m/s. Determine R and C such that the contacts will be protected. [$C > 0.1$ μF, $200\,\Omega < R < 500\,\Omega$]

REFERENCES

1. C. R. Paul and S. A. Nasar, *Introduction to Electromangetic Fields*, 2nd edn., McGraw-Hill, New York, 1987.
2. C. R. Paul and W. W. Everett, III, *Lumped Model Approximations of Transmission Lines: Effect of Load Impedances on Accuracy*, Technical Report, Rome Air Development Center, Griffiss AFB, NY, RADC-TR-82-286, Vol. IV. E (Aug. 1984).
3. J. C. Clements, C. R. Paul, and A. T. Adams, Two-dimensional systems of dielectric-coated, cylindrical conductors, *IEEE Trans. Electromagn. Compat.* **EMC-17**, 238–248 (1975).
4. C. R. Paul, *Fundamentals of Electric Circuit Analysis*, Wiley, New York, 2001.
5. C. R. Paul, *Analysis of Linear Circuits*, McGraw-Hill, New York, 1989.

6. H. W. Ott, *Noise Reduction Techniques,* In *Electronic Systems*, 2nd edn., Wiley-Interscience, New York, 1988.
7. J. C. Englebrecht and K. Hermes, *A Study of Decoupling Capacitors for EMI Reduction*, Technical Report, International Business Machines, TR-51.0152, May 1984.
8. D. M. Hanttula and S. W. Wong, Case study—effect of analog buffer amplifier on radiated emissions, *Proc. 1985 IEEE Int. Symp. Electromagnetic Compatibility,* Wakefield, MA, Aug. 1985.
9. C. R. Paul, S. A. Nasar, and L.E. Unnewehr, *Introduction to Electrical Engineering*, McGraw-Hill, New York, 1986.
10. D. R. Kerns, Integrated circuit construction and its effect on EMC performance, *Proc. 1984 IEEE Symp. Electromagnetic Compatibility*, San Antonio, TX, April 1984.
11. R. Holm, *Electric Contacts, Theory and Application*, 4th edn., Springer-Verlag, Berlin, 1967.
12. H. N. Wagar, Performance principles of switching contacts, *Physical Design of Electronic Systems*, Vol. 3. *Integrated Device and Connection Technology* (Bell Laboratories), Prentice-Hall, Englewood Cliffs, NJ, 1971, Chapter 9.
13. J. D. Cobine, *Gaseous Conductors*, Dover, New York, 1958.
14. A. M. Curtis, Contact phenomena in telephone switching circuits, *Bell Syst. Tech. J.* **19**, 40–62 (1940).
15. G. W. Mills, The mechanism of the showering arc, *IEEE Trans. Parts, Mater. Pack.,* **PMP-5**, 47–55 (1969).
16. E. K. Howell, How switches produce electrical noise, *IEEE Trans. Electromagn. Compat.* **EMC-21**, 162–170 (1979).
17. S. A. Hall, C. R. Paul, K. B. Hardin, and A. E. Nielsen, Prediction of crosstalk due to showering arcs at switch contacts, *Proc. 1991 IEEE Int. Symp. Electromagnetic Compatability*, Cherry Hill, NJ, Aug. 1991.

CHAPTER SIX

Conducted Emissions and Susceptibility

In this chapter we will investigate the mechanism by which emissions are generated and are conducted out of the product along the product's ac power cord. Regulatory agencies impose limits on these *conducted emissions* because they are placed on the commercial power system net of the installation. The commercial power distribution system in an installation is a large array of wires connecting the various power outlets from which the other electronic systems in the installation receive their ac power. It therefore represents a large "antenna" system from which these conducted emissions can radiate quite efficiently, causing interference in the other electronic systems of the installation. Thus the conducted emissions may cause radiated emission, which may then cause interference. Ordinarily, the reduction of these conducted emissions is somewhat simpler than the reduction of radiated emissions since there is only one path for these emissions that needs to be controlled: the unit's power cord. However, it is important to realize that *if a product fails to comply with the limits on conducted emissions, compliance with the limits on radiated emissions is a moot point*! Therefore controlling conducted emissions of a product has equal priority with the control of radiated emissions.

Once again, manufacturers of electronic products realize that simply complying with the regulatory limits on conducted and radiated emissions does not represent a complete design from the standpoint of EMC. A product must be reasonably insensitive to disturbances that are present on the power system net in order to ensure reliable operation of the product. For example, lightning may strike the power transmission lines that feed power to the installation. This may cause disturbances that range from a complete loss of commercial power (which no product is expected to withstand) to momentary power loss due to power system circuit breakers attempting to reclose (which a product is expected to withstand without loss of

Introduction to Electromagnetic Compatibility, *Second Edition*, by Clayton R. Paul